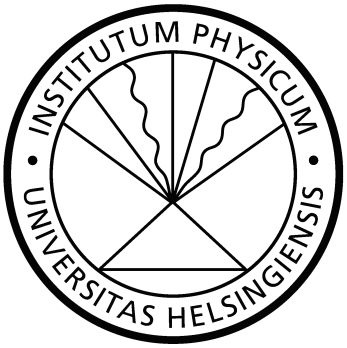

Master's thesis
Theoretical physics

A Model of Composite Dark Matter in Light-Front Holographic QCD

Jere Remes
2015

Advisor: Kimmo Tuominen
Examiners: Kimmo Tuominen
Aleksi Vuorinen

UNIVERSITY OF HELSINKI
DEPARTMENT OF PHYSICS

PL 64 (Gustaf Hällströmin katu 2)
00014 University of Helsinki

HELSINGIN YLIOPISTO — HELSINGFORS UNIVERSITET — UNIVERSITY OF HELSINKI

Tiedekunta/Osasto — Fakultet/Sektion — Faculty	Laitos — Institution — Department
Faculty of Science	Department of Physics

Tekijä — Författare — Author

Jere Remes

Työn nimi — Arbetets titel — Title

A Model of Composite Dark Matter in Light-Front Holographic QCD

Oppiaine — Läroämne — Subject

Theoretical physics

Työn laji — Arbetets art — Level	Aika — Datum — Month and year	Sivumäärä — Sidoantal — Number of pages
Master's thesis	August 2015	87

Tiivistelmä — Referat — Abstract

Even after 50 years, there is still no standard, analytically tractable way to treat Quantum Chromodynamics (QCD) non-numerically besides perturbation theory. In the high-energy regime perturbation theory agrees with experimental results to a great accuracy. However, at low energies the theory becomes strongly coupled and therefore not computable by perturbative methods. Therefore, non-perturbative methods are needed, and one of the candidates is light-front holography.

In this thesis, the basics of light-front quantisation and holography are discussed. Light-front quantisation takes light-cone coordinates and the Hamiltonian quantisation scheme as its basis and the resulting field theory has many beneficial properties like frame-independence. Still, to extract meaningful results from the light-front QCD, one needs to apply bottom-up holographic methods.

Last part of this work focuses on the applicability of light-front holographic QCD in the area of dark matter. We find that one can build a secluded SU(3) sector consisting of a doublet of elementary particles, analogous to quarks and gluons. Due to a global symmetry, the lightest stable particle is analogous with ordinary neutron. It meets the basic requirements for being a WIMP candidate when its mass is higher than 5 TeV.

Avainsanat — Nyckelord — Keywords

holography, light-front holography, QCD, dark matter

Säilytyspaikka — Förvaringsställe — Where deposited

Kumpula campus library

Muita tietoja — Övriga uppgifter — Additional information

Contents

Kiitokset

Opiskeluvuodet Helsingin yliopistolla ovat olleet elämäni rikkaimpia vuosia sekä ympäristön, matkustamisen, taiteen, tieteen että ennen kaikkea ihmisten takia. Siksi onkin tarpeen osoittaa kiitokseni teille yhteisesti.

Ensiksi haluaisin kiittää ohjaajaani Kimmo Tuomista tämän työn mainiosta ohjauksesta, aiheen esittämisestä ja valaisevista keskusteluista. On myös aihetta kiittää Aleksi Vuorista tämän työn tarkastamisesta. Lisäksi tämän tutkielman sisältöön vaikuttivat maininnan arvoisesti omilta osiltaan Tommi Tenkanen ja Eemeli Tomberg auttaessaan erään matemaattisen kynnyksen ylittämisessä ja Johann Muszynski antaessaan tärkeää palautetta tästä behemotista. Jarkko Järvelää ja Alexander Meaneyta taas on kiittäminen vertaistuesta työn synkempinä hetkinä.

Tuntuisi vähättelyltä alkaa eritellä opiskelutovereitani nimin kiitokseen: mikäli olette joskus pudonneet seinältä seuranani tai istuneet pöytään kanssani miettimään olevaisen luonnetta missään muodossa – fyysisessä kuin metafyysisessä – olette ansainneet syvimmät kiitokseni, sillä mikään ei ole niin elähdyttävää kuin älyllinen keskustelu.

Lisäksi haluan muistaa perhettäni opintoihin kannustamisesta ja kasvattamisestani. On ollut etuoikeus saada kasvaa niin moninaisessa ja tiiviissä perhepiirissä kuin muodostamamme on ollut.

Suurimmat kiitokset kuuluvat Katjalle sietämisestäni ja järjissä pitämisestäni. Enempää en osaa tekstualisoida tähän.

> Minä sanon teille: täytyy vielä sisältää kaaosta voidakseen synnyttää tanssivan tähden. Minä sanon teille: teissä on vielä kaaosta.
>
> F. Nietzsche, *Näin puhui Zarathustra*

Notations and conventions

In this thesis, *natural units* are used, i.e. $\hbar = c = 1$. Also, the Minkowski metric tensor η is realised in the mostly minus form

$$\eta^{\mu\nu} = \mathrm{diag}(1, -1, -1, -1). \tag{1}$$

The basic AdS_{d+1} metric is in the form

$$\mathrm{d}s^2 = \frac{R^2}{z^2}\left(\eta_{\mu\nu}\,\mathrm{d}x^\mu\,\mathrm{d}x^\nu - \,\mathrm{d}z^2\right), \tag{2}$$

where the Greek letters denote the Lorentz indices of the d-dimensional spacetime $\mu, \nu = 0, \ldots, d$. The vielbeins for AdS_{d+1} are

$$e^A_M = \frac{R}{z}\delta^A_M, \tag{3}$$

where $M = 0, \ldots, d$ are the AdS indices and $A = 0, \ldots, d$ are the AdS tangent space indices.

For the rank-J tensors in AdS_{d+1} the notations $\Phi_{\{N\}}$ and $\Phi_{\{LN_{/j}\}}$ are used, where

$$\Phi_{\{N\}} = \Phi_{N_1 N_2 \ldots N_J} \tag{4}$$

$$\Phi_{\{LN_{/j}\}} = \Phi_{LN_1 \ldots N_{j-1} N_{j+1} \ldots N_J}, \tag{5}$$

and a similar notation is used for the products of components of the metric g^{MN}:

$$g^{\{MN\}} = g^{M_1 N_1} \cdots g^{M_J N_J}. \tag{6}$$

In light-front the Lepage-Brodsky (LB) convention [1] is used:

$$x^\mu = (x^+, x^-, x^1, x^2) = (x^+, x^-, \mathbf{x}_\perp), \tag{7}$$

$$x^+ = x^0 + x^3, \tag{8}$$

$$x^- = x^0 - x^3, \tag{9}$$

where the x^0 and x^i are the Minkowski coordinates ($i = 1, 2, 3$). The flat metric is then

$$g^{\mu\nu} = \begin{pmatrix} 0 & 2 & 0 & 0 \\ 2 & 0 & 0 & 0 \\ 0 & 0 & -1 & 0 \\ 0 & 0 & 0 & -1 \end{pmatrix}, \quad g_{\mu\nu} = \begin{pmatrix} 0 & \frac{1}{2} & 0 & 0 \\ \frac{1}{2} & 0 & 0 & 0 \\ 0 & 0 & -1 & 0 \\ 0 & 0 & 0 & -1 \end{pmatrix}. \tag{10}$$

In the LB convention the new Dirac matrices in Dirac representation become

$$\gamma^+\gamma^+ = \gamma^-\gamma^- = 0 \tag{11}$$

and the projection operators are thus

$$\Lambda_+ = \frac{1}{2}\gamma^0\gamma^+ = \frac{1}{4}\gamma^-\gamma^+, \tag{12}$$

$$\Lambda_- = \frac{1}{2}\gamma^+\gamma^- = \frac{1}{4}\gamma^+\gamma^-. \tag{13}$$

The volume integral in the LB convention is

$$\int \mathrm{d}\omega_+ = \frac{1}{2}\int \mathrm{d}x^- \, \mathrm{d}^2x_\perp = \int \mathrm{d}x_+ \, \mathrm{d}^2x_\perp, \tag{14}$$

where the raising and lowering of the Lorentz indices is done with

$$\epsilon_{+12}{}^{+} = 1 \tag{15}$$

$$\Rightarrow \epsilon_{+12-} = \frac{1}{2}. \tag{16}$$

The light-front spinors are

$$u(p,\lambda) = \frac{1}{\sqrt{p^+}}\left(p^+ + \gamma^0 m + \gamma^0\gamma^k p_{\perp k}\right) \times \begin{cases} \chi(\uparrow) \text{ for } \lambda = +1 \\ \chi(\downarrow) \text{ for } \lambda = -1 \end{cases} \tag{17}$$

$$v(p,\lambda) = \frac{1}{\sqrt{p^+}}\left(p^+ + \gamma^0 m - \gamma^0\gamma^k p_{\perp k}\right) \times \begin{cases} \chi(\downarrow) \text{ for } \lambda = +1 \\ \chi(\uparrow) \text{ for } \lambda = -1, \end{cases} \tag{18}$$

where $k = 1, 2, 3$ and

$$\chi(\uparrow) = \frac{1}{\sqrt{2}}\begin{pmatrix} 1 \\ 0 \\ 1 \\ 0 \end{pmatrix}, \qquad \chi(\downarrow) = \frac{1}{\sqrt{2}}\begin{pmatrix} 0 \\ 1 \\ 0 \\ -1 \end{pmatrix}. \tag{19}$$

To avoid confusion between Euler's constant e and electromagnetic coupling constant e, the latter is always in italics.

Chapter 1

Introduction

Quantum chromodynamics (QCD)– the SU(3) gauge field theory of quarks and gluons – has been proven by time to be the correct theory of strong interactions. Perturbative QCD predicts a great variety of high-energy scattering results with great success. However, because of its strongly coupled nature, no perturbative predictions can be made for low energies, and therefore there is still no analytical demonstration of colour confinement, hadron mass spectrum or other crucial details of the theory. Important aspects on that end have been shown by numerical Euclidean lattice methods. But even as lattice QCD has been hugely successful in many cases, aspects of QCD, such as the excitation spectrum of light hadrons, is still a formidable challenge because of its computational complexity.

It would be of a great theoretical advantage to have an analytically calculable form of the theory for closer examination of its properties like the mass spectrum. There is still no standard, analytically tractable way to handle quantum field theories besides perturbation theory. To find one, it is probable that we need to make an analytical, relativistic, non-perturbative approximation of the wanted model, which can then be improved upon. One of the possible methods for achieving an approximation of QCD is using *light-front holography* – a light-cone quantised formulation of QCD dual to a gravity theory.

Light-cone quantisation was found by P. A. M. Dirac in 1949 [2]. It takes light-cone coordinates $x^+ = x^0 - x^3$ as the new time coordinate, and uses a

Hamiltonian quantisation scheme instead of the usual action quantisation. These simple changes result in a fully relativistic, frame-independent, ghost-free formulation of the field theory. Because the vacuum has a simple structure, the light-front wave functions (LFWFs) can be defined unambiguously. The wave functions $|\psi\rangle$ of a bound state can be obtained from the eigenvalue equation $H_{LF}\,|\psi\rangle = \mathcal{M}^2\,|\psi\rangle$, which becomes an infinite set of coupled integral equations for the Fock-state expansion. Here an approximation is made to solve the equation, and only the valence state is taken into account. Still, the solution is lacking the interaction term, which cannot be retrieved from pure QCD. This is where holographic methods are needed.

Holographic models utilise the AdS/CFT duality. It is a conjectured duality between type IIb string theory in $\mathrm{AdS}_5\times\,\mathrm{S}^5$ and conformal $\mathcal{N}=4$ super Yang-Mills gauge field theory, first put forward by Juan Maldacena in his seminal 1997 article [3]. It has been a source of renewed interest in string theories for the past 18 years. Not only is the duality seen as a possible route to a fundamental theory of everything, but also as a way to analyse strongly coupled systems because of its strong/weak-type duality. Therefore QCD would have a weakly coupled string theory – a classical theory of gravity – as its dual theory.

In this thesis we look also into the applicability of the light-front holographic QCD by constructing a model of composite dark matter consisting of a secluded SU(3) sector particles analogous to quarks and gluons. The elementary particles of the model interact with the standard model via the electroweak force, but the lightest stable particle in the model, which is the neutron-analogue because of isospin symmetry, is electroweak-neutral.

This thesis is organised as follows. In Chapter 2, the basic notions of holography and AdS/CFT duality are handled in a pragmatic manner to give a general impression of the ideas that form the basis for the holographic model used in Chapter 3.

In Chapter 3, the problems of QCD are handled with an approach based on light-front quantisation and holography. First we look at a broad overview on the experimental evidence for QCD, what the theoretical problems using perturbative QCD are, and what light-front quantisation is. Then, we use the semi-classical approximation to build a holographic model of QCD and

calculate observables like the mass spectra of pseudoscalar mesons, vector mesons and baryons, form factors for the pion and nuclei and their charge radius and magnetic moment.

In Chapter 4 "the dark matter problem" is discussed and light-front holographic QCD is applied to it as a possible solution by adding a secluded sector to the Standard Model and having the secluded model interact with Standard Model particles via the electroweak channel. We discover that a dark matter particle analogous to neutron would need to have a mass of the order of 5 TeV to satisfy the exclusions from the XENON100 experiment.

Chapter 2

Basics of Gauge/Gravity Duality

In this Chapter a brief and a rather pragmatic overview is given on string theory and holography. Light-front holography does not rigorously use the AdS/CFT conjecture but uses it rather as an inspiration. So, to understand the main subject of the thesis, only the very basics of the holographic principle and AdS/CFT correspondence (or in our case, *gauge/gravity correspondence*) are needed. For a deeper take on the subjects, Bousso's article [4] on holography and Aharony et al's article [5] on AdS/CFT are recommended.

2.1 The Holographic Principle

To understand the AdS/CFT duality we need to discuss the basics of the *holographic principle* – i.e. that a d dimensional space time can be fully described by a $d-1$ dimensional hypersurface. The idea of holography came about by Gerard 't Hooft in 1993 [6] as an attempt to solve the information paradox, and it was later developed upon by Charles Thorn [7] – who actually discussed the possibility before 't Hooft – and Leonard Susskind [8].

The information paradox arises when one considers objects falling into a black hole. Quantum mechanics requires that at a local scale one has discrete degrees of freedom and the evolution laws of the system must be reversible to allow superposition. But if we have no way of recovering a particle that has

fallen into a black hole, we have lost reversibility and information.

However, it is possible to argue that any object falling into a black hole leaves some signal behind in our world in an unknown way. The Bekenstein-Hawking entropy of a black hole is [9, 10]

$$S = \frac{A}{4G_d}, \tag{2.1}$$

where G_d is Newton's constant in d dimensions and A is the area of the horizon. This entropy is also the Bekenstein limit for maximum entropy inside a boundary. The formula, being dependent on area instead of volume, suggests that the information about the black hole is somehow encoded in the boundary instead of the bulk of the black hole. And in fact, using the quantum mechanical "third law of thermodynamics", which states that the number of possible states $\mathcal{N}$ is related to the entropy as $\mathcal{N} = e^S$, one can try to match the degrees of freedom: if one has a system with n spins having two possible values, we get [4, 6]

$$n = \frac{A}{4G \log 2}. \tag{2.2}$$

Following this logic, 't Hooft argues that the observable degrees of freedom inside any closed surface can be described with Boolean variables defined on a lattice on that surface, evolving in time. The analogue of this is a hologram of a three-dimensional object on a two-dimensional surface, where all the information regarding the three-dimensional image is encoded on the two-dimensional surface.

Klebanov and Susskind [11] and Thorn [7] have concluded independently that a superstring theory can be written as a $2+1$-dimensional theory.

2.2 Type IIb Strings on AdS_5

2.2.1 Anti-de Sitter Space

Before going into the conjectured duality between the type IIb superstring theory on $\mathrm{AdS}_5 \times \mathrm{S}^5$ and $\mathcal{N} = 4$ conformal SU(N) super Yang-Mills (SYM), we need to define what we mean by both.

Firstly, a $d+1$-dimensional anti-de Sitter space (AdS_{d+1}) is a maximally symmetric vacuum solution of Einstein equations

$$R_{\mu\nu} - \frac{1}{2} g_{\mu\nu}\mathcal{R} + g_{\mu\nu}\Lambda = 0, \tag{2.3}$$

when the cosmological constant Λ is negative. The fact that it is a maximally symmetric Lorentzian manifold requires that it has $(d+2)(d+1)/2$ symmetries [12]. One way to define the metric of AdS_{d+1} is

$$\mathrm{d}s^2 = \frac{R^2}{z^2}\left(\eta_{\mu\nu}\,\mathrm{d}x^\mu\,\mathrm{d}x^\nu - \,\mathrm{d}z^2\right), \tag{2.4}$$

where η is the metric tensor of the d-dimensional Minkowski space, $z \in \mathbb{R}^+$, and R is the curvature radius defined as

$$R^2 = \frac{-d(d-1)}{2\Lambda}, \tag{2.5}$$

so that the embedding of AdS_{d+1} into a $d+2$-dimensional Minkowski space with metric $\eta_{ab} = \mathrm{diag}(1, -1, -1, \ldots, -1, 1)$ has to satisfy

$$(x^0)^2 - \sum_{i=1}^{d}(x^i)^2 + (x^{d+1})^2 = R^2. \tag{2.6}$$

The global symmetry group of the AdS_{d+1} space is $\mathrm{SO}(d,2)$ – this fact plays a central role in gaining a heuristic understanding of the duality.

2.2.2 Type IIb String Theory

String theory was first formulated to model the strong interactions, but it had some problems such as having non-observed spin-2 particles. As QCD proved to be the sustaining theory of strong interactions, string theory fell out of fashion. But instead of dying out, it found a new life as a unified theory with the spin-2 state identified as the graviton.

String theories come in five flavours: types I, IIa and IIb, and Heterotic SO(32) and $\mathrm{E}_8\times\ \mathrm{E}_8$. In every string theory, instead of point-like particles being the fundamental objects of the theory, one-dimensional strings are. One can get rid of the extra dimensions of the theories by compactifying them.

Type IIb superstring theory has objects called *D-branes* plus open and closed strings. D-branes are massive, dynamical objects to which open strings

are attached to via Dirichlet boundary conditions and they are also the solitonic solutions to supergravity (SUGRA) in ten dimensions. Open strings are one-dimensional objects that can be massless or massive, and the different oscillations of the strings correspond to different particles and describe the excitations of the D-branes. The closed strings are not attached to branes and correspond to a massless spin-2 state – a graviton. They are excitations of space-time itself. [5]

At energy scales below $1/l_s$, l_s being the string length, only massless strings are excitable. The closed strings give a gravity supermultiplet in ten dimensions and the lower energy effective Lagrangian is thus a IIb SUGRA Lagrangian, whereas the open strings have a low-energy Lagrangian of $\mathcal{N} = 4$, U(N) SYM. [5, 13]

2.3 AdS/CFT

2.3.1 Conformal Field Theory

First, let us define what we mean by a *conformal field theory* (CFT). A CFT is simply a quantum field theory which is invariant under a class of conformal transformations – mappings which preserve angles locally. We can define the conformal mapping C between two pseudo-Riemannian manifolds (M, g) and (M', g') to be a smooth mapping with a property

$$C^* g' = \Omega^2 g, \tag{2.7}$$

where $\Omega : M \to \mathbb{R}^+$ is a smooth, positive function [14]. In practice, the transformation is simply $g \to g' = \Omega^2(x)g$. The symmetry group of these transformations in d dimensions is SO(2,d), exactly matching the symmetry group of the $d+1$ dimensional AdS_{d+1} space. The symmetry group comprises of the Poincaré transformations, scaling transformations $x^\mu \to \lambda x^\mu$, $\lambda \in \mathbb{R}$ and special conformal transformations, i.e. symmetry under coordinate transformations

$$x^\mu \to \frac{x^\mu - b^\mu x^2}{1 - 2x_\mu b^\mu - b^2 x^2}, \tag{2.8}$$

where $b^\mu \in M^d$ [5].

Because of the scaling invariance, a CFT must not have any dimensional parameters such as gauge coupling or mass. However, de Alfaro, Fubini and Furlan [15] showed that a mass scale can be introduced to the Hamiltonian without breaking the conformal invariance of a 1+1-dimensional field theory. Also, a theory can be classically conformal, but quantum effects break the invariance by generating a mass scale via self-interactions – QCD can be viewed as an example of such a theory.

2.3.2 AdS/CFT Correspondence

Here the conjecture is justified on the basis of heuristic arguments. For a more rigorous motivation see e.g. references [3, 5, 16]. One needs to remember, that the correspondence is still a conjecture: despite the seemingly strong evidence backing the conjecture and the fact that no counterexamples have been found, there is still no rigorous proof of the duality.

The conjecture by Maldacena is in its strongest form as follows. The type IIb superstring theory living on $\mathrm{AdS}_{d+1}\times\ \mathrm{S}^5$ is the same as the conformal Yang-Mills SU(N) gauge field theory with four supersymmetric charges living on the boundary of the AdS space. The fact that both theories have the same symmetries and number of states lends the conjecture credibility. The SYM in four dimensions has the conformal symmetry group SO(4,2) and a global R-symmetry SU(4)$\simeq$SO(6). $\mathrm{AdS}_5\times\mathrm{S}^5$ has the total symmetry group of SO(4,2)$\times$SO(6), so the symmetries match.

The simplest formulation of the AdS/CFT correspondence in $d = 4$ is that the partition functions of the theories agree on the conformal boundary,

$$Z_{\mathrm{CFT}}[\phi_0] = \int \mathcal{D}\mathcal{O}\mathrm{e}^{iS_{\mathrm{CFT}}[\mathcal{O}]+i\int \mathrm{d}^4x\phi_0\mathcal{O}} = Z_{\mathrm{AdS}}[\phi(x, z \to 0) = \phi_0(x)], \quad (2.9)$$

where $\mathcal{O}$ is an operator of the CFT, ϕ_0 is a source in CFT and $\phi(x, z)$ is a field in AdS. [16, 17]

There are weaker formulations of the correspondence, stating that the theories are only dual if N is large. Let us define the 't Hooft coupling $\lambda = g^2_{\mathrm{YM}}N = g_sN$, where g_{YM} is the Yang-Mills coupling, g_s is the string coupling and N is the number of colors. If one takes the large-N limit keeping the coupling λ constant one has a classical string theory on the AdS side and

an N^{-1} expansion of the Yang-Mills on the CFT side. If we on the other hand take the large 't Hooft limit and let $\lambda \to \infty$, we will have a classical supergravity and a strongly coupled Yang-Mills.

The gravity description of the string theory is a viable approximation when the string length ℓ_s is much smaller than the curvature radius R of the AdS and S spaces, as ℓ_s is also the intrinsic size of the graviton [18].

Once we establish a dictionary between these two theories, we can translate the calculations done in one realm to another. Therefore, for every scalar field ϕ in AdS, there is a scalar operator $\mathcal{O}$ in CFT, for every gauge field A_μ, there is a current J_μ, and for every metric $g_{\mu\nu}$, there is an energy-momentum tensor $T_{\mu\nu}$.

As we work on the light-front holographic model of QCD, we are taking advantage of the fact that a strongly coupled CFT is dual to a weakly coupled string theory. This makes computations in the AdS realm considerably simpler, as the weakly coupled limit of type IIb string theory proves to be classical supergravity, which is a lot easier to solve than quantum gravity or the strongly coupled dual theory. Still, we cannot use the AdS/CFT duality *per se* as QCD is not a CFT.

2.4 Holography Bottom-up

There are some major issues one needs to address when using the AdS/CFT holographic approach: gravity seems to be four-dimensional and no field theory known to describe Nature is a CFT – the Standard Model has a mass scale and running couplings, strong interactions are confined, and we have seen no supersymmetric particles to date.

We may still be able to use the duality and build models that agree with our standard model on the boundary – we can use holography as a tool to calculate difficult problems in the more easily solvable gravity regime. There are basically two approaches to building a holographic model: *top-down* and *bottom-up*.

In the top-down approach one tries to look for a superstring theory with a low-energy limit of the brane configuration corresponding to a known field theory. The positive side of this approach is that both theories are well known

and the duality between them can be argued for easily. The negative side is that finding the right string theory that corresponds to any of the standard model interactions without any additional gauge groups is hard.

The bottom-up approach to holography is more phenomenological of an approach: one takes a known field theory and constructs an approximate gravity theory on a higher dimensional space corresponding to the known theory. Then the theory is usually non-supersymmetric and non-conformal, and thus justifying the duality is difficult. Still, this way the models can be built upon a phenomenological basis and complex strongly coupled systems can be solved in a non-perturbative manner. For bottom-up models AdS/CFT correspondence can be viewed more as a motivation, not a rigid basis.

Chapter 3

Light Front Holography

3.1 The Problem with Strong Interactions

3.1.1 Experimental Evidence of QCD

QCD exhibits some properties not present in Abelian gauge field theories, e.g. asymptotic freedom and confinement. Asymptotic freedom – the decrease of the strong coupling constant $\alpha_s(Q)$ as the energy scale Q increases – was shown analytically to be true for non-Abelian gauge field theories by Politzer [19], Wilczek and Gross [20] in 1973. [21, 22] In the one-loop approximation, one expects the coupling constant to evolve as

$$\frac{1}{\alpha_s(Q)} = \frac{1}{\alpha_s(\mu)} + \frac{33 - 2n_f}{6\pi} \log\left(\frac{Q}{\mu}\right) \tag{3.1}$$

where μ sets the renormalisation scale and n_f is the number of quark flavours [23].

The world average of the experimental results at the common scale $\mu = M_Z$ is $\alpha_s(M_Z) = 0.1184 \pm 0.0007$ and the QCD prediction on the four-loop level can be fitted with this average value so that the predicted evolution of the coupling closely matches the observed behaviour [23, 24]. The results are summarised in Figure 3.1.

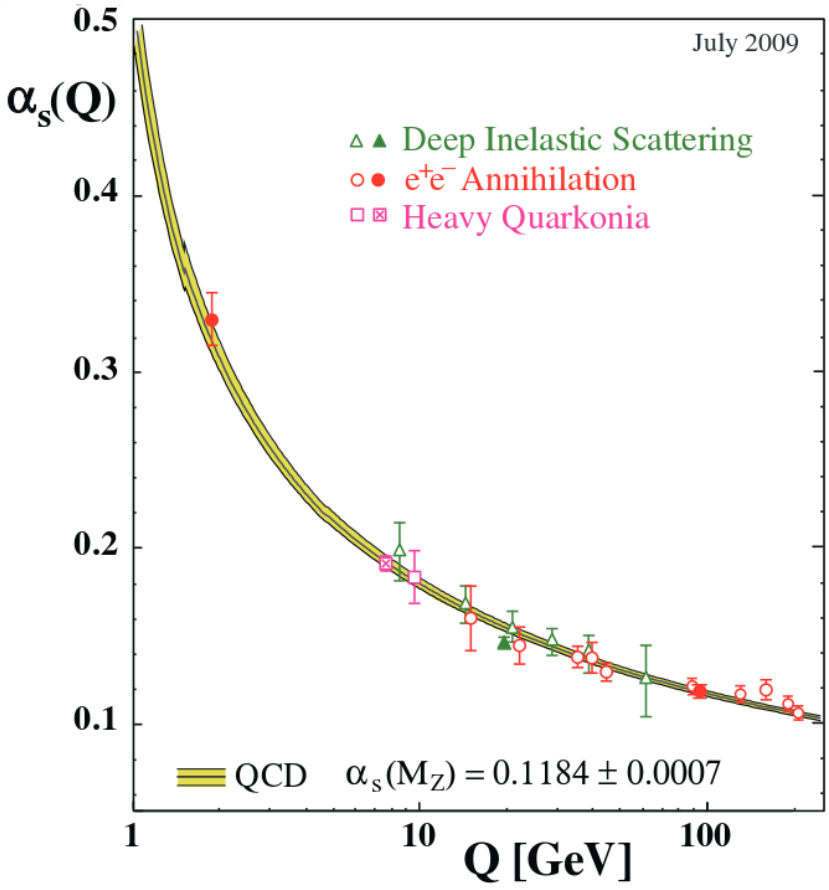

Figure 3.1: Summary of the α_s measurements. The curve is the QCD prediction determined by choosing $\Lambda_{\bar{M}S}$ so that it fits the average result. Source [23]

Because the coupling constant decreases with the energy scale, perturbative methods can used in the high-energy regime. One of the predictions in this scale is the ratio R between the cross sections of $e^+e^- \to$ hadrons and $e^+e^- \to \mu^+\mu^-$. There is a rough agreement with the results and the three-loop calculation of such processes. [24]

One can also use the e^+e^- collisions to study the group-theory structure of strong interactions, because various observables are sensitive to different combinations of quark and gluon colour factors C_F and C_A respectively. As QCD is SU(3) gauge symmetric, one expects these factors to be $C_F = \frac{4}{3}$ and $C_A = 3$, and LEP gives $C_F = 1.30 \pm 0.09$ and $C_A = 2.89 \pm 0.21$ which are in excellent agreement with the theory. The results are summarised in

Figure 3.2. [25]

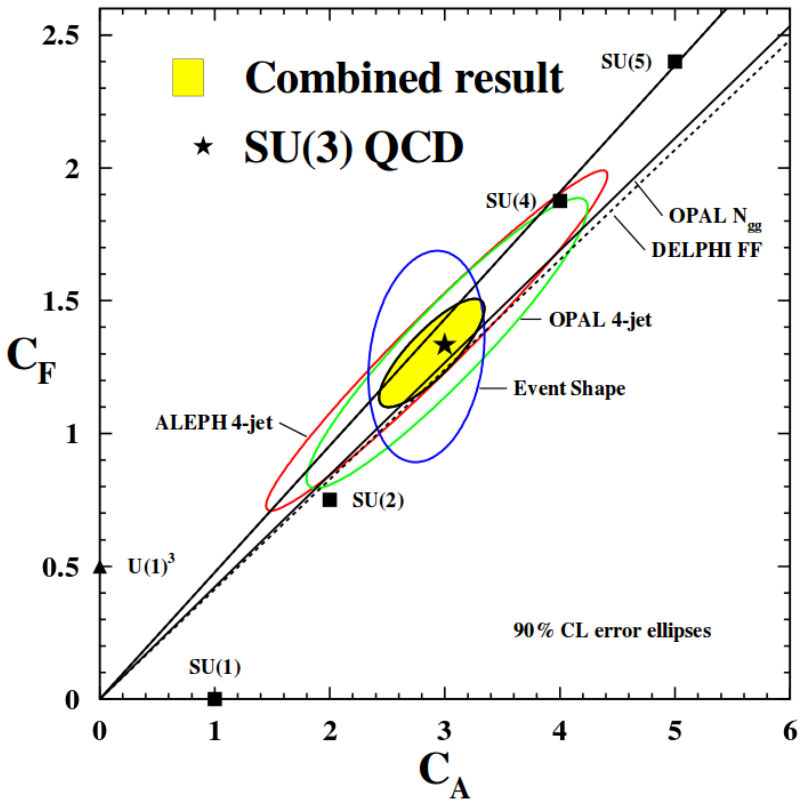

Figure 3.2: Determination of the colour factors from e^+e^- collisions. Source [25]

The results of high energy $\bar{p}p$ to dijet reactions studied at Tevatron with center of mass energies up to $\sqrt{s} = 1.96$ TeV agree well with the predictions from perturbative QCD (pQCD), evaluated at next-to-leading order [26]. These results are summarised in Figure 3.3. The ATLAS collaboration has presented similar results for $\sqrt{s} = 2.76$ TeV and have concluded that pQCD predictions are in good agreement with the data and describe jet production at high jet transverse momentum [27].

There are of course more examples backing up QCD, such as deep inelastic scattering (DIS) or the Drell-Yan process [28]. For a comprehensive review of pQCD methods and a summary of the results from Tevatron, see reference [29].

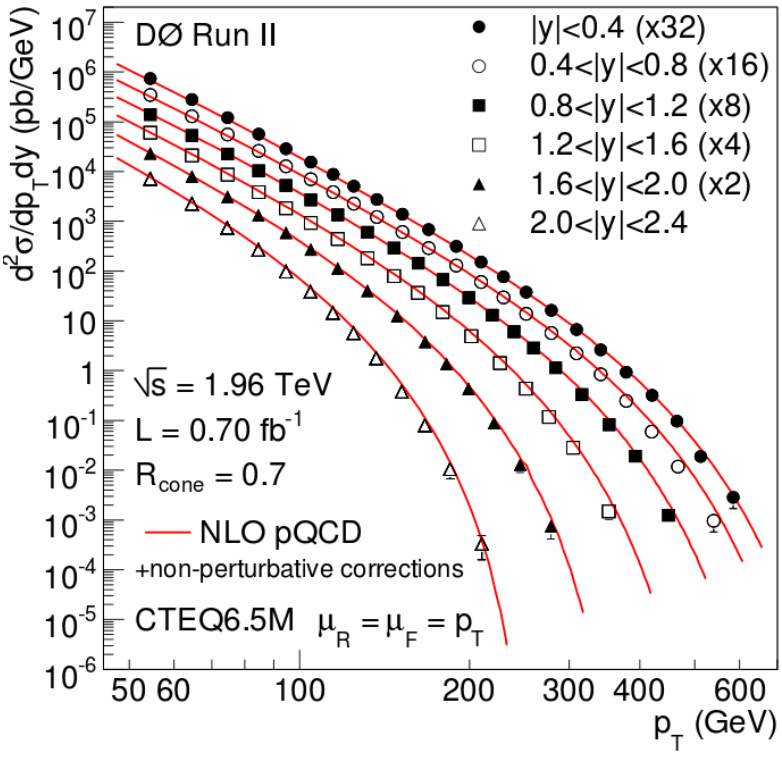

Figure 3.3: Tevatron D0 results for inclusive jet cross section as a function of the transverse momenta p_T for six different bins of jet rapidities y. Source [26]

3.2 Light-Cone Quantisation

As mentioned before, QCD is strongly coupled in the low-energy regime. This makes the analytical calculation of the low-energy processes nearly impossible as the usual perturbative methods fail, and one has to think of new ways of extracting predictions from the theory by formulating the theory anew.

Although lattice QCD has been successful in extracting relevant information computationally, it would be of a great theoretical advantage to find some analytical description of strong interactions and having a complementary approach to QCD. Furthermore, reformulating existing theories has previously paved way to building new ones.

One way of obtaining non-perturbative solutions of QCD is to use *light cone quantisation*.

Dirac was the first to find the three fundamental forms of Hamiltonian

dynamics; the *instant form*, the *point form* and the *front form*. For illustrations of these different frames, see Figure 3.4. The instant form is the conventional choice when doing relativistic field theory and the point form is still investigated relatively little. Here we focus on the front form. [1, 2]

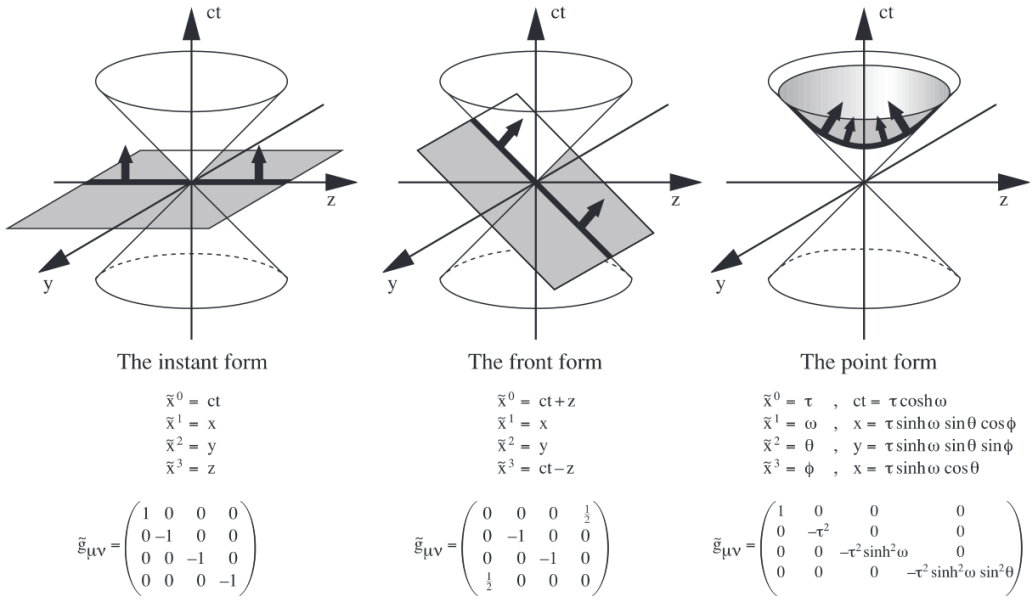

Figure 3.4: The three forms of Relativistic Dynamics. Source [1]

3.2.1 The Hamiltonian Quantisation Scheme

The approach explored in this thesis is based on quantising the Hamiltonian instead of the action. Normally one uses the action approach, as it is especially handy when computing cross sections, which are easily measured in experiments. The Hamiltonian approach is a lot less used, but it is proven to be a useful take when computing bound states.

The Hamiltonian operator P_0 can be defined in relativistic field theory as [1]

$$P_0 \left|x^0\right\rangle = i\frac{\partial}{\partial x^0}\left|x^0\right\rangle, \tag{3.2}$$

and this is practically unchanged in the light front

$$P_+ \left|x^+\right\rangle = i\frac{\partial}{\partial x^+}\left|x^+\right\rangle, \tag{3.3}$$

where the light-cone time x^+ is defined in terms of regular Minkowski coordinates as follows:

$$\begin{aligned} x^+ &= x^0 + x^3, \\ x^- &= x^0 - x^3. \end{aligned} \tag{3.4}$$

Thereby $\partial_+ = \frac{1}{2}\partial^-$ is a time-like and $\partial_- = \frac{1}{2}\partial^+$ a space-like derivative. The metric tensor $g_{\mu\nu}$ is

$$g_{\mu\nu} = \begin{pmatrix} 0 & \frac{1}{2} & 0 & 0 \\ \frac{1}{2} & 0 & 0 & 0 \\ 0 & 0 & -1 & 0 \\ 0 & 0 & 0 & -1 \end{pmatrix}. \tag{3.5}$$

If one defines the contravariant four vectors as $x^\mu = (x^+, x^-, x^1, x^2)$, the scalar product looks like $a \cdot b = g_{\mu\nu} a^\mu b^\nu = \frac{1}{2}(a^+ b^- + a^- b^+) - a^1 b^1 - a^2 b^2$.

The normal vector for hypersurface $\Sigma : x^+ = 0$ is $N^\mu = (0, 1, 0, 0)$ in the light-front coordinates, and the unit vector along the x^+ direction is $n^\mu = (1, 0, 0, 0)$, so that $n \cdot N = 1$. The Hamiltonian is now

$$\begin{aligned} H_{x^+} &= n \cdot p = \frac{p^-}{2} \\ &= \frac{p_\perp^2 + m^2}{2p^+} \end{aligned} \tag{3.6}$$

which, unlike in the instant form, does not contain a square root.

Let us now construct the Poincaré algebra for free massive particles with a constraint $p^2 = m^2$ and setting $x^+ = 0$: we have the kinematical generators

$$\begin{aligned} P^i = p^i, \qquad & P^+ = p^+ \\ M^{+i} = -x^i p^+, \qquad & M^{12} = x^1 p^2 - x^2 p^1, \quad M^{+-} = -x^- p^+, \end{aligned} \tag{3.7}$$

where the momenta P correspond to transverse and longitudinal translations within the hypersurface Σ, the M^{+i} correspond to transverse rotations, the M^{12} to rotations around the z-axis, and M^{+-} to boosts in the z-direction. These seven kinematical operators are the largest stability group (a group of transformations that leaves Σ invariant) among Dirac's forms of dynamics, as the usual formulation only has six of them [2]. [30]

The dynamical operators, or the ones that transform the hypersurface Σ to another, say Σ', and thus generate development in x^+ and are associated with the Hamiltonian, are then

$$P^- = \frac{p_\perp^2 + m^2}{p^+} = 2H_{x^+}, \qquad M^{-i} = x^- p^i - x^i p^-. \tag{3.8}$$

However, the discussion of the Poincaré algebra in the free case with a fixed number of particles will not suffice, as we do not wish to formulate a quantum mechanical theory of free particles, but a dynamical quantum field theory with interacting fields. Luckily, one can construct the four-momentum P^μ and the generalized angular momentum $M^{\mu\nu}$ using the energy-momentum tensor $T^{\mu\nu} = \dfrac{\partial \mathcal{L}}{\partial(\partial_\mu \phi)} \partial^\nu \phi - g^{\mu\nu}\mathcal{L}$, where ϕ denotes any field that the Lagrangian depends on:

$$P^\mu = \frac{1}{2} \int \mathrm{d}x^- \, \mathrm{d}^2 x^\perp T^{+\mu} \tag{3.9}$$

$$M^{\mu\nu} = \frac{1}{2} \int \mathrm{d}x^- \, \mathrm{d}^2 x^\perp \left(x^\nu T^{+\mu} - x^\mu T^{+\nu} \right) \tag{3.10}$$

and their Poincaré algebra is

$$[P^\mu, P^\nu] = 0, \tag{3.11}$$

$$[P^\mu, M^{\rho\sigma}] = i \left(g^{\mu\rho} P^\sigma - g^{\mu\sigma} P^\rho \right), \tag{3.12}$$

$$[M^{\mu\nu}, M^{\rho\sigma}] = i \left(g^{\mu\sigma} M^{\nu\rho} - g^{\mu\rho} M^{\nu\sigma} - (\mu \leftrightarrow \nu) \right) \tag{3.13}$$

where $\mu \leftrightarrow \nu$ marks the exchange of indices μ to indices ν and vice versa. And as before, P^- is the Hamiltonian, the other P's are the momenta, the M^{+i} and M^{+-} are boosts and $M^{12} = J^3$ and M^{-i} are rotations. [30, 31]

The QCD Lagrangian is

$$\mathcal{L}_{\mathrm{QCD}} = \bar{\psi}(i\gamma^\mu D_\mu - m)\psi - \frac{1}{4} G^a_{\mu\nu} G^{a\ \mu\nu} \tag{3.14}$$

where $D_\mu = \partial_\mu - i g_s A^a_\mu T^a$, $G^a_{\mu\nu} = \partial_\mu A^a_\nu - \partial_\nu A^a_\mu + g_s c^{abc} A^b_\mu A^c_\nu$, the T^a are the $SU(3)_C$ generators, c^{abc} are the corresponding structure constants and a, b, c

are colour indices. So the Poincaré generators of the theory are

$$P^- = \frac{1}{2}\int \mathrm{d}x^-\,\mathrm{d}^2x^\perp \bar{\psi}_+\gamma^+\frac{(i\nabla_\perp)^2+m^2}{i\partial^+}\psi_+ + \text{interactions} \quad (3.15)$$

$$P^+ = \int \mathrm{d}x^-\,\mathrm{d}^2x^\perp \bar{\psi}_+\gamma^+ i\partial^+\psi_+ \quad (3.16)$$

$$\mathbf{P}_\perp = \frac{1}{2}\int \mathrm{d}x^-\,\mathrm{d}^2x^\perp \bar{\psi}_+\gamma^+ i\nabla_\perp\psi_+ \quad (3.17)$$

where the Dirac field is projected as $\psi_\pm = \Lambda_\pm\psi$, with the projection operator defined as $\Lambda_\pm = \gamma^0\gamma^\pm$, and using the $A^+ = 0$ gauge, which results in the elimination of Faddeev-Popov and Gupta-Bleuler ghosts and makes the gluon polarization purely transverse [32–34]. [35]

The Dirac field operator in the light-front is

$$\psi_+(x)_\alpha = \sum_\lambda \int_{q^+>0} \frac{\mathrm{d}q^+\,\mathrm{d}^2\mathbf{q}_\perp}{(2\pi)^3\sqrt{2q^+}}\left[b_\lambda(q)u_\alpha(q,\lambda)e^{-iqx} + d^\dagger_\lambda(q)v_\alpha(q,\lambda)e^{iqx}\right], \quad (3.18)$$

where u and v are spinors presented in Chapter 1 and the creation and annihilation operators $b, b^\dagger, d$ and $d^\dagger$ obey the anticommutation relation

$$\left\{b(q), b^\dagger(q')\right\} = \left\{d(q), d^\dagger(q')\right\} = (2\pi)^3\delta(q^+ - q'^+)\delta^{(2)}(\mathbf{q}_\perp - \mathbf{q}'_\perp). \quad (3.19)$$

Thereby, the generator P^- can be written as

$$P^- = \sum_\lambda \int \frac{\mathrm{d}q^+\,\mathrm{d}^2\mathbf{q}_\perp}{(2\pi)^3}\frac{m^2+\mathbf{q}_\perp^2}{q^+}b^\dagger_\lambda(q)b_\lambda(q) + \text{interactions}. \quad (3.20)$$

One of the advantages of the light-front formulation is the trivial structure of the QCD vacuum. The conventional vacuum is defined as the lowest energy eigenstate at a given time x^0 everywhere in $\mathbf{x}$ resulting to the vacuum being acausal and frame-dependent. So, to avoid causal violations, one needs to normal-order the operators before doing any calculations. In light-front, however, the vacuum is defined as the eigenstate with the lowest invariant mass at fixed x^+ over all x^- and $\mathbf{x}_\perp$. It is still frame-dependent, but causal. [34]

The vacuum structure is further simplified by the fact that all particles have positive momentum k^+, and the + momentum is conserved. This results in normal vacuum bubbles being kinematically forbidden and thus

QCD vacuum is trivial up to a possible zero mode (a mode with zero four-momentum). Thus we have no quark or gluon condensates in the vacuum and we can define the partonic content of a hadron unambiguously: all the physics is in the light-front wave functions. [34]

3.3 Modelling Hadrons

As mentioned previously, we do not observe free partons in the low-energy regime - we observe hadrons. Therefore it is of utmost importance to extract the needed information out of our theory of strong interactions. A novel approach to achieve this was developed by Erlich, Katz, Son and Stephanov [36] and independently by Da Rold and Pomarol [37], inspired by AdS/CFT correspondence. It was later developed into *light-front holography* by Brodsky and de Téramond [38]. In this section the semi-classical light-front wave equation is built upon the basis of LFQCD developed in the previous section. Then, for much needed extra information on the confining potential, an effective gravity dual for LFQCD is built to find this potential.

3.3.1 Light-Front Wave Equation for Mesons

The hadronic eigenstates $|\psi\rangle \equiv |\psi(P^+, \mathbf{P}_\perp, J^z)\rangle$ can be expanded in a complete Fock-state basis of non-interacting n-particle states $|n\rangle$: $|\psi\rangle = \sum_n \psi_n |n\rangle$, where $\psi_n \equiv \psi_n(x_i, \mathbf{k}_{\perp\, i}, \lambda_i)$ are the light-front wave functions (LFWFs) with $x_i = k_i^+/P^+$ being the momentum fractions of the partons compared to the total momentum P^+. Thus they obey $\sum_{i=1}^n x_i = 1$, as $\sum_{i=1}^n k_i^+ = P^+$, and the λ_i being the spins components of respective particles. The new variables defining the LFWFs are independent of P being frame-independent and thus the LFWFs are boost-invariant. [32, 35]

The strongly correlated bound-state problem can be approximated using the invariant mass of the constituents in each n-particle Fock-state $\mathcal{M}_n^2 = (k_1 + k_2 + \ldots k_n)^2$, or

$$\mathcal{M}_n^2 = \sum_{i=1}^{n} \frac{\mathbf{k}_{\perp i}^2 + m_i^2}{x_i}. \tag{3.21}$$

Now, as $P_\mu P^\mu = \mathcal{M}^2$,

$$H_{LF}\,|\psi\rangle = \mathcal{M}^2\,|\psi\rangle\,. \tag{3.22}$$

The computation of the total mass squared $\mathcal{M}^2$ is simplified in the frame $P = (P^+, P^-, \mathbf{0})$, because then $P^2 = P^+P^- = \mathcal{M}^2 \Rightarrow P^- = \mathcal{M}^2/P^+$, in a naïve notation. The boost to the $\mathbf{P}_\perp = 0$ frame does not affect the result, as the LFWFs are boost-invariant. Now we find

$$\begin{aligned}
\mathcal{M}^2 &= \sum_n \int [\,\mathrm{d}x_i][\,\mathrm{d}^2\mathbf{k}_{\perp i}] M_n^2 |\psi_n(x_i \mathbf{k}_{\perp\ i})|^2 + \text{interactions} \\
&= \sum_n \int [\,\mathrm{d}x_i][\,\mathrm{d}^2\mathbf{k}_{\perp i}] \sum_q \left(\frac{\mathbf{k}_{\perp\ q}^2 + m_q^2}{x_q} \right) |\psi_n(x_i \mathbf{k}_{\perp\ i})|^2 \\
&\quad + \text{interactions},
\end{aligned} \tag{3.23}$$

with similar terms for antiquarks and gluons. The integrals in equation (3.23) are defined as [35]

$$\begin{aligned}
\int [\,\mathrm{d}x_i] &= \prod_{i=i}^{n} \int_0^1 \mathrm{d}x_i\ \delta\left(1 - \sum_{j=1}^{n} x_j\right), \\
\int [\,\mathrm{d}^2\mathbf{k}_{\perp i}] &= \prod_{i=1}^{n} \int \mathrm{d}^2\mathbf{k}_{\perp i}\ \delta^{(2)}\left(\sum_{j=1}^{n} \mathbf{k}_{\perp j}\right),
\end{aligned} \tag{3.24}$$

with the normalisation

$$\sum_n \int [\,\mathrm{d}x_i][\,\mathrm{d}^2\mathbf{k}_{\perp i}] |\psi_n(x_i, \mathbf{k}_{\perp i})|^2 = 1. \tag{3.25}$$

This can be simplified by adopting a mixed representation, expressing the LFWFs in terms of the $n-1$ independent position coordinates $\mathbf{b}_{\perp j}$ conjugate to $\mathbf{k}_{\perp i}$, with $\sum_{i=1}^n \mathbf{b}_{\perp i} = 0$. After identifying $\mathbf{k}_{\perp j}^2 \to -\nabla^2_{\mathbf{b}_{\perp j}}$, and seeing, that the wave functions transform as [39]

$$\psi_n(x_i, \mathbf{k}_{\perp i}) = (4\pi)^{(n-1)/2} \prod_{j=1}^{n-1} \int \mathrm{d}^2\mathbf{b}_{\perp j}\ \exp\left[i \sum_{k=1}^{n-1} \mathbf{b}_{\perp k} \cdot \mathbf{k}_{\perp k} \right] \psi_n(x_j, b_{\perp j}), \tag{3.26}$$

the equation (3.23) can be written as

$$\begin{aligned}
\mathcal{M}^2 &= \sum_n \prod_{j=1}^{n-1} \int \mathrm{d}x_j\, \mathrm{d}^2\mathbf{b}_{\perp j} \psi_n^*(x_j, \mathbf{b}_{\perp j}) \sum_q \left(\frac{-\nabla^2_{\mathbf{b}_{\perp q}} + m_q^2}{x_q} \right) \psi_n(x_j, \mathbf{b}_{\perp j}) \\
&\quad + \text{interactions}.
\end{aligned} \tag{3.27}$$

One could try to solve the mass for all n, but that proves to be quite a difficult feat. To simplify the discussion, following references [40] and [35], let us take the first semi-classical approximation, $n = 2$, for a meson. This means that there will be no quantum effects, as the only contributions to the hadronic wave function come from the valence Fock state. [41]

Now, for $n = 2$, the only value j can take is 1, $q = 2$ and $x_1 \equiv x$, $x_2 = 1-x$. In the chiral limit $m_q \to 0$, $\mathcal{M}^2$ becomes

$$\begin{aligned} \mathcal{M}^2 &= \int_0^1 \frac{\mathrm{d}x}{x(1-x)} \int \mathrm{d}^2\mathbf{b}_\perp \psi^*(x,\mathbf{b}_\perp)(-\nabla^2_{\mathbf{b}_\perp})\psi(x,\mathbf{b}_\perp) \\ &\quad +\text{interactions.} \end{aligned} \tag{3.28}$$

By changing variables and switching to cylindrical coordinates, we can introduce a transverse impact variable ζ representing the invariant separation of quarks at $x^+ =$ constant, and defined as

$$\zeta^2 = x(1-x)\mathbf{b}_\perp^2. \tag{3.29}$$

Separating the differential equation we can write

$$\psi(x,\zeta,\theta) = \mathrm{e}^{iL\theta} X(x) \frac{\phi(\zeta)}{\sqrt{2\pi\zeta}}, \tag{3.30}$$

where the longitudinal dependence is in $X(x)$, which separates only in the $m_q \to 0$ limit [42], and θ is the angle of $\mathbf{b}_\perp$ in cylindrical coordinates, which is factored out using the SO(2) Casimir representation L^2 of the orbital angular momentum in the transverse plane. The Laplacian now reads

$$\nabla^2_\zeta = \frac{1}{\zeta}\frac{\mathrm{d}}{\mathrm{d}\zeta}\left(\zeta\frac{\mathrm{d}}{\mathrm{d}\zeta}\right) + \frac{1}{\zeta^2}\frac{\partial^2}{\partial\theta^2}. \tag{3.31}$$

Putting everything together, Equation (3.28) can now be written as

$$\begin{aligned} \mathcal{M}^2 &= \int \mathrm{d}\zeta\phi^*(\zeta)\sqrt{\zeta}\left(-\frac{\mathrm{d}^2}{\mathrm{d}\zeta^2} - \frac{1}{\zeta}\frac{\mathrm{d}}{\mathrm{d}\zeta} + \frac{L^2}{\zeta^2} + U(\zeta)\right)\frac{\phi(\zeta)}{\sqrt{\zeta}} \\ &= \int \mathrm{d}\zeta\phi^*(\zeta)\left(-\frac{\mathrm{d}^2}{\mathrm{d}\zeta^2} - \frac{1-4L^2}{4\zeta^2} + U(\zeta)\right)\phi(\zeta). \end{aligned} \tag{3.32}$$

Rewriting $P^\mu P_\mu |\phi\rangle = \mathcal{M}^2 |\phi\rangle$ is now simple and results in the light-front wave equation (LFWE)

$$\left(-\frac{\mathrm{d}^2}{\mathrm{d}\zeta^2} - \frac{1-4L^2}{4\zeta^2} + U(\zeta)\right)\phi(\zeta) = \mathcal{M}^2\phi(\zeta), \tag{3.33}$$

where all the interactions are encoded in the effective potential $U(\zeta)$. This potential has still not been tractable from the first principles of QCD, and thus one needs to obtain additional information in order to solve the equation. Luckily we can retrieve the potential through the gauge/gravity correspondence, which is quite remarkable when you come to think of the approximations made.

3.3.2 The Duality

QCD is a Yang-Mills gauge field theory, not a conformal super-Yang-Mills theory, so one cannot use the AdS/CFT correspondence as it is. One can still take a bottom-up approach in building a viable gravitational dual model, as we do know that QCD is nearly conformal in the $m_q \to 0$ approximation in the strongly coupled regime [40].

The holographic methods on the light-front were first introduced by showing explicitly that there is a mapping between the Polchinski-Strassler formula [43] for the electromagnetic form factors in AdS space and the corresponding Drell-Yan-West formula [44, 45] at fixed light-front time in LFQCD [35]. Since then, an identical mapping has been found between the energy-momentum tensors of the weakly coupled gravity theory on AdS and the strongly coupled LFQCD [35] and their corresponding form factors [46, 47]. As explained in chapter 2, we expect to find a mapping between the operators of our 4 dimensional, semiclassical field theory and the fields in 5 dimensional gravity theory.

We start from QCD and build a viable, simple, non-stringy Lagrangian in the AdS_5 realm, retaining the symmetries of QCD. This is most easily done by making an ansatz, recovering the equations of motion and then making an explicit mapping between the two theories.

One must make sure the AdS dual is a confined theory, and this is incorporated in the gauge/gravity correspondence by modifying the AdS geometry by setting a scale for strong interactions in the IR domain. This is possible, as the AdS metric is invariant under a dilatation of coordinates, and thus the additional dimension z acts as a scaling variable in Minkowski space setting the different energy scales [35]. The truncation of the metric can

be done either by introducing a cut-off at some value $z_0 \sim \Lambda_{\mathrm{QCD}}^{-1}$, called the *hard-wall* method, or by introducing a dilaton field $\varphi(z)$ to smoothly truncate the metric exponentially (the *soft-wall* method). Here we consider generally the case with dilaton. The hard-wall scenario is obtainable as a special case $\varphi = 0$.

3.3.3 Effective Potential

Taking after reference [42], let us try to find the effective potential to compliment the equation (3.32) using an effective action,

$$S_{\mathrm{eff}} = \int \mathrm{d}^4x\,\mathrm{d}z\,\sqrt{|g|}\mathrm{e}^{\varphi(z)}g^{\{NN'\}}\left(g^{MM'}D_M\Phi^*_{\{N\}}D_{M'}\Phi_{\{N'\}} - \mu(z)^2_{\mathrm{eff}}\Phi^*_{\{N\}}\Phi_{\{N'\}}\right), \tag{3.34}$$

on the AdS_5 side for rank-J tensor field $\Phi(x^M)_{\{N\}}$ representing the integer spin field. The 5 dimensional mass function $\mu(z)_{\mathrm{eff}}$ is *a priori* unknown and is a function of the energy scale z to separate the kinematical and dynamical effects as we will soon discover. The Christoffel symbols Γ^L_{MN} for AdS_5 are

$$\Gamma^L_{MN} = -\frac{1}{z}\left(\delta^z_M\delta^L_N + \delta^z_N\delta^L_M - \eta^{Lz}\eta_{MN}\right), \tag{3.35}$$

and the covariant derivatives D_M are

$$\begin{aligned} D_M\Phi_{\{N\}} &= \partial_M\Phi_{\{N\}} - \sum_j \Gamma^L_{MN_j}\Phi_{\{LN_{/j}\}} \qquad (3.36)\\ &= \partial_M\Phi_{\{N\}} + \frac{1}{z}\sum_j\left(\delta^z_M\Phi_{\{N_jN_{/j}\}} + \delta^z_{N_j}\Phi_{\{MN_{/j}\}} + \eta_{MN_j}\Phi_{\{zN_{/j}\}}\right). \end{aligned}$$

It seems now sensible to move to the local tangent frame, as

$$\begin{aligned} \hat{\Phi}_{\{A\}} &= e^{\{N\}}_{\{A\}}\Phi_{\{N\}} \\ &= \left(\frac{z}{R}\right)^J\Phi_{\{A\}}. \end{aligned} \tag{3.37}$$

The vielbeins and tangent frame are more carefully scrutinized in section 3.3.4.

The z-derivative simplifies to

$$D_z\Phi_{\{N\}} = \left(\frac{R}{z}\right)^J\partial_z\hat{\Phi}_{\{N\}}. \tag{3.38}$$

And the original μ-derivative,

$$D_\mu \Phi_{\{N\}} = \partial_\mu \Phi_{\{N\}} + \frac{1}{z} \sum_j \eta_{\mu N_j} \Phi_{\{zN_{/j}\}}, \tag{3.39}$$

can be written as

$$g^{\mu\mu'} g^{\{\nu\nu'\}} D_\mu \Phi^*_{\{\nu\}} D_{\mu'} \Phi_{\{\nu'\}} = g^{\mu\mu'} \eta^{\{\nu\nu'\}} \left(\partial_\mu \hat{\Phi}^*_{\{\nu\}} \partial_{\mu'} \hat{\Phi}_{\{\nu'\}} + g^{zz} \frac{J}{z^2} \hat{\Phi}^*_{\{\nu\}} \hat{\Phi}_{\{\nu'\}} \right), \tag{3.40}$$

since $g^{\mu\nu} = z^2/R^2 \ \eta^{\mu\nu}$. One can now rewrite the effective action and drop out terms quadratic in Φ that have one or more indices z, as one expects the physical particles to have polarisation indices only in the direction of the non-holographic dimensions. I.e. $\Phi_{\{zN_{/j}\}} = 0$ and thus the quadratic terms do not contribute to the Euler-Lagrange equations. The remainder of the effective action can be written as a sum of terms $S^{[0]}_{\text{eff}}$ not containing the z index, and terms $S^{[1]}_{\text{eff}}$ linear in fields $\Phi^*_{\{zN_{/j}\}}$, as we wish to vary the action with respect to $\Phi^*_{\{N\}}$.

The two remaining parts of the effective action are

$$\begin{aligned} S^{[0]}_{\text{eff}} \ = \ & \int \mathrm{d}^d x \, \mathrm{d}z \left(\frac{R}{z}\right)^{d-1} \mathrm{e}^{\varphi(z)} \eta^{\{\nu\nu'\}} \left(-\partial_z \hat{\Phi}^*_{\{\nu\}} \partial_z \hat{\Phi}_{\{\nu'\}} + \eta^{\mu\mu'} \partial_\mu \hat{\Phi}^*_{\{\nu\}} \partial_{\mu'} \hat{\Phi}_{\{\nu'\}} \right. \\ & \left. - \left[\left(\frac{\mu_{\text{eff}}(z) R}{z} \right)^2 + J\Omega^2(z) \right] \hat{\Phi}^*_{\{\nu\}} \hat{\Phi}_{\{\nu'\}} \right), \end{aligned} \tag{3.41}$$

where – following reference [42] – the trivial factors z^{-1} are separated from the warp factors $\Omega(z) = z^{-1}$ resulting from the affine connection, and the other term is

$$\begin{aligned} S^{[1]}_{\text{eff}} \ = \ & \int \mathrm{d}^d x \, \mathrm{d}z \left(\frac{R}{z}\right)^{d-1} \mathrm{e}^{\varphi(z)} J\Omega(z) \left(-\eta^{\mu\mu'} \eta^{\{N_{/1}\nu'_{/1}\}} \partial_\mu \hat{\Phi}^*_{\{zN_{/1}\}} \hat{\Phi}_{\{\mu'\nu'_{/1}\}} \right. \\ & + \eta^{\mu\nu} \eta^{\{N_{/1}\nu'_{/1}\}} \hat{\Phi}^*_{\{zN_{/1}\}} \partial_\mu \hat{\Phi}_{\{\nu\nu'_{/1}\}} \\ & \left. - (J-1)\Omega(z) \eta^{\mu\nu} \eta^{N_3\nu'_3} \cdots \eta^{N_J\nu'_J} \hat{\Phi}^*_{zzN_3\ldots N_J} \hat{\Phi}_{\mu\nu\nu'_3\ldots\nu'_J} \right). \end{aligned} \tag{3.42}$$

The term $S^{[1]}_{\text{eff}}$ can now be disregarded: the affine connection is explicitly present in all the terms, and it thus only contributes to kinematical constraints.

Varying the action (3.41) with respect to $\hat{\Phi}^*_{\{\nu\}}$, one arrives at the quite familiar looking equation of motion in the local tangent frame:

$$\left(\partial^\mu \partial_\mu - \frac{z^{d-1}}{\mathrm{e}^{\varphi(z)}} \partial_z \left(\frac{\mathrm{e}^{\varphi(z)}}{z^{d-1}} \partial_z \right) + \frac{(\mu_{\text{eff}}(z) R)^2 + J}{z^2} \right) \hat{\Phi}_{\{\nu\}} = 0, \tag{3.43}$$

which translates into the general frame in terms of $\Phi_{\{\nu\}}$ as

$$\left(\partial^\mu\partial_\mu - \frac{z^{d-1-2J}}{\mathrm{e}^{\varphi(z)}}\partial_z\left(\frac{\mathrm{e}^{\varphi(z)}}{z^{d-1-2J}}\partial_z\right) + \frac{(\mu R)^2}{z^2}\right)\Phi_{\{\nu\}} = 0, \tag{3.44}$$

where μ is the rescaled five-dimensional mass

$$(\mu R)^2 = (\mu_{\mathrm{eff}}R)^2 - Jz\varphi'(z) + J(d-J+1). \tag{3.45}$$

To solve Equation (3.44), let us write the tensor as a product of the plane wave solution $\mathrm{e}^{iP\cdot x}$, a polarisation vector $\epsilon_{\{\nu\}}$ and explicitly z dependent function $\Phi_J(z)$:

$$\Phi_{\{\nu\}}(x,z) = \mathrm{e}^{iP\cdot x}\Phi_J(z)\epsilon_{\{\nu\}}(P), \tag{3.46}$$

with normalisation

$$R^{d-1-2J}\int_0^\infty \frac{\mathrm{d}z}{z^{d-1-2J}}\mathrm{e}^{\varphi(z)}\Phi_J^2(z) = 1. \tag{3.47}$$

$P^\mu P_\mu = \mathcal{M}^2$ can be used to write the equation (3.44) as

$$\left(-\frac{z^{d-1-2J}}{\mathrm{e}^{\varphi(z)}}\partial_z\left(\frac{\mathrm{e}^{\varphi(z)}}{z^{d-1-2J}}\partial_z\right) + \frac{(\mu R)^2}{z^2}\right)\Phi_J = \mathcal{M}^2\Phi_J. \tag{3.48}$$

Now we can define the explicit light-front holographic mapping between LFQCD$_{3+1}$ and AdS$_5$ by taking

$$z = \zeta, \tag{3.49}$$

$$\Phi_J(z) \equiv \Phi_J(\zeta) = \left(\frac{\zeta}{R}\right)^{3/2-J}\mathrm{e}^{-\varphi(\zeta)/2}\phi_J(\zeta), \tag{3.50}$$

with ϕ_J being the LFWF. The equation of motion (3.48) can be written as

$$\left(-\frac{\mathrm{d}^2}{\mathrm{d}\zeta^2} - \frac{1-4L^2}{4\zeta^2} + U(\zeta)\right)\phi_J(\zeta) = \mathcal{M}^2\phi_J(\zeta), \tag{3.51}$$

in $d=4$ after some tedious but straightforward algebra, with the effective potential

$$U(\zeta) = \frac{1}{2}\varphi''(\zeta) + \frac{1}{4}\varphi'(\zeta)^2 + \frac{2J-3}{2\zeta}\varphi'(\zeta), \tag{3.52}$$

and provided that the fifth dimensional mass μ obeys the dispersion relation

$$(\mu R)^2 = -(2-J)^2 + L^2, \tag{3.53}$$

with the internal orbital angular momentum being $L = \max|L^z|$ and the total angular momentum $J^z = L^z + S^z$.

The equation (3.51) is exactly the LFWE (3.33), with the effective potential (3.52), which could not be recovered from QCD.

3.3.4 Light Front Wave Equation for Baryons

The mesonic case can be more or less straightforwardly adapted into the more complicated case of spin-1/2 baryons, once we find out how to get to the five-dimensional Dirac equation. However, the light-front wave equation is not formally derived in this case, but rather tailor-made to match the AdS equations of motion.

The Covariant Derivative of a Spinor in AdS Space

In Riemannian geometry, when a particle moves along a closed curve, the tangent vector is parallel transported and it changes accordingly. But when we introduce a spin to the particle, this is not sufficient - when the space has torsion, the spin changes. So, we need to introduce the *vielbein* formalism to determine the *spin connection*.

First, the Dirac matrices Γ_M in five flat dimensions are supposed to fulfil the anticommutation relation

$$\{\Gamma_A, \Gamma_B\} = 2\eta_{AB}. \tag{3.54}$$

This is easily seen to be fulfilled by a set of the usual gamma matrices

$$\Gamma_M = (\gamma_\mu, -i\gamma_5). \tag{3.55}$$

Thus, in AdS_5, the matrices should be

$$\tilde{\Gamma}_M = \frac{R}{z}\Gamma_M, \tag{3.56}$$

as this yields the correct anticommutation relation

$$\left\{\tilde{\Gamma}_A, \tilde{\Gamma}_B\right\} = 2g_{AB}, \tag{3.57}$$

$$= 2\frac{R^2}{z^2}\eta_{AB}. \tag{3.58}$$

A vielbein e^α is a set of vector fields defined on a (pseudo-)Riemannian manifold, such that at a given point P with coordinates ζ^α in a Minkowski frame can be written in terms of the coordinates x^μ of the general frame with metric tensor $g_{\mu\nu}(x)$:

$$e^\alpha_\mu = \partial_\mu \zeta^\alpha. \tag{3.59}$$

This results in a relation

$$\eta_{\alpha\beta} e^{\alpha}_{\mu} e^{\beta}_{\nu} = g_{\mu\nu}, \tag{3.60}$$

and thus the vielbein can be seen as a connection between the inertial frame and the general frame. [12] For AdS_5 the vielbeins are thus

$$e^{A}_{M} = \frac{R}{z} \delta^{A}_{M}. \tag{3.61}$$

The spin connection $\omega^{\alpha\beta}_{\mu}$, which tells how the vielbein behaves when transported, can be deduced from the fact that the complete covariant derivative of the vielbein should vanish,

$$D_\mu e^{\alpha}_{\nu} = \partial_\mu e^{\alpha}_{\nu} - \Gamma^{\lambda}_{\mu\nu} e^{\alpha}_{\lambda} + \omega^{\alpha}_{\mu\beta} e^{\beta}_{\nu} = 0. \tag{3.62}$$

Multiplying the equation by $g^{\nu\rho} e^{\gamma}_{\rho}$ and using the inverse vielbeins for equation (3.60) we end up with

$$\begin{aligned} 2\omega^{\alpha\gamma}_{\mu} &= g^{\nu\nu'} \left(e^{\gamma}_{\nu'} e^{\alpha}_{\lambda} \Gamma^{\lambda}_{\mu\nu} - e^{\gamma}_{\nu'} \partial_\mu e^{\alpha}_{\nu} \right) - (\alpha \leftrightarrow \gamma) \\ \Leftrightarrow \omega^{\alpha\beta}_{\gamma} &= \frac{1}{2} \left(e^{\alpha}_{\nu} \partial_\mu g^{\nu\nu'} e^{\beta}_{\nu'} + e^{\alpha}_{\nu} g^{\sigma\sigma'} e^{\beta}_{\sigma'} \Gamma^{\nu}_{\sigma\mu} - (\alpha \leftrightarrow \beta) \right). \end{aligned} \tag{3.63}$$

For AdS_5 the only non-vanishing spin connections are

$$\omega^{5\alpha}_{\mu} = -\omega^{\alpha 5}_{\mu} = \frac{1}{z} \delta^{\alpha}_{\mu}, \tag{3.64}$$

where $\alpha, \mu = 0, \ldots, 3$.

Disregarding the gauge field for now, we can define the covariant derivative of a spinor ψ in a general, smooth manifold, as

$$D_\mu \psi = \left(\partial_\mu + \frac{i}{4} \omega^{\alpha\beta}_{\mu} \sigma_{\alpha\beta} \right) \psi, \tag{3.65}$$

the $\sigma_{\alpha\beta}$ being the generators for Lorentz transformations

$$\sigma_{\alpha\beta} = \frac{1}{2i} \left[\gamma_\alpha, \gamma_\beta \right]. \tag{3.66}$$

Again, for AdS_5 the generators Σ_{AB} are

$$\Sigma_{AB} = \frac{1}{2i} \left[\Gamma_A, \Gamma_B \right], \tag{3.67}$$

and the covariant derivative reduces to

$$D_M = \partial_M + \frac{i}{4z}\left(\Sigma_{5M} - \Sigma_{M5}\right), \tag{3.68}$$

or

$$\begin{aligned} D_\mu &= \partial_\mu - \frac{1}{2z}\Gamma_\mu\Gamma_5, & (3.69)\\ D_5 &= \partial_z. & (3.70) \end{aligned}$$

Effective Action in AdS Space

Following e.g. reference [48], the effective action for spin-1/2 baryons in AdS_5 for both the positive and negative dilaton is taken to be

$$\begin{aligned} S^{\pm}_{1/2} &= \int \mathrm{d}^4x\,\mathrm{d}z\sqrt{g}\mathrm{e}^{\pm\varphi(z)}\left[\frac{i}{2}\bar{\Psi}(x,z)e^M_a\Gamma^a D_M\Psi(x,z)\right. & (3.71)\\ &\left. -\frac{i}{2}\left(D_M\Psi(x,z)\right)^\dagger\Gamma^0 e^M_a\Gamma^a\Psi(x,z) - \bar{\Psi}(x,z)\left(\mu + V_F(z)\right)\Psi(x,z)\right], \end{aligned}$$

where $\mu R = \Delta - d/2$. Δ is the dimension of the baryon interpolating operator. It relates to the twist τ as $\Delta = \tau + S = \tau + 1/2$. [48]

In this case, we notice the dilaton field can be scaled away by rescaling the Ψ field:

$$\Psi(x,z) \to \mathrm{e}^{\mp\varphi(z)/2}\Psi(x,z). \tag{3.72}$$

After rescaling, both possible sign choices share the same φ-independent action,

$$\begin{aligned} S_{1/2} &= \int \mathrm{d}^4x\,\mathrm{d}z\sqrt{g}\left[\frac{i}{2}\bar{\Psi}(x,z)e^M_a\Gamma^a D_M\Psi(x,z)\right. & (3.73)\\ &\left. -\frac{i}{2}\left(D_M\Psi(x,z)\right)^\dagger\Gamma^0 e^M_a\Gamma^a\Psi(x,z) - \bar{\Psi}(x,z)\left(\mu + V_F(z)\right)\Psi(x,z)\right]. \end{aligned}$$

Thus, to break the conformal invariance, we need to introduce the dilaton into the effective potential instead of modifying the metric. This is most easily done by taking V_F to be $V_F = \varphi(z)/R$ as our confining potential. We will also see that this reproduces the linear Regge behaviour of mass.

The action is now

$$S_{1/2} = \int \mathrm{d}^4x\,\mathrm{d}z\sqrt{g}\bar{\Psi}(x,z)\left[i\Gamma^M\partial_M - \frac{2}{z}\gamma^5 - \frac{1}{z}(\mu R + \varphi(z))\right]\Psi(x,z). \tag{3.74}$$

The corresponding equations of motion (the $5d$ Dirac equations) for variation with respect to $\bar{\Psi}$ are thus

$$\begin{aligned} \left[i\Gamma^M\partial_M - \frac{2}{z}\gamma^5 - \frac{1}{z}(\mu R + \varphi(z))\right]\Psi(x,z) &= 0 \\ \Leftrightarrow \left[iz\partial\!\!\!/ + \gamma^5 z\partial_z - 2\gamma^5 - \mu R - \varphi(z)\right]\Psi(x,z) &= 0. \end{aligned} \tag{3.75}$$

One can now separate the left- and right-handed solutions as

$$\Psi_{L/R} = \frac{1 \pm \gamma^5}{2}\Psi \tag{3.76}$$

$$\Rightarrow \gamma^5\Psi_{L/R} = \mp\Psi_{L/R}, \tag{3.77}$$

$$\Psi = \Psi_L + \Psi_R, \tag{3.78}$$

and make a Kaluza-Klein expansion of the solutions

$$\Psi_{L/R} = \sum_n F^n_{L/R}(x)\Psi^n_{L/R}(z). \tag{3.79}$$

Now the EOM (3.75) is a pair of coupled PDEs:

$$\left[\partial_z \pm \frac{\mu R + \varphi(z)}{z} - \frac{2}{z}\right]\Psi^n_{L/R} = \pm\mathcal{M}\Psi^n_{R/L}, \tag{3.80}$$

where we have used the Dirac equation $i\partial\!\!\!/ F^n_{L/R} = \mathcal{M}_n F^n_{R/L}$ for the Minkowski solutions. The equations can be easily decoupled by differentiating both sides. We can also substitute $\Psi^n_{L/R} = z^2\psi^n_{L/R}$ to get

$$\left[-\partial_z^2 + \frac{(\mu R + \varphi)^2}{z^2} \pm \frac{\mu R + \varphi}{z^2} \mp \frac{1}{z}\frac{\mathrm{d}}{\mathrm{d}z}\varphi\right]\psi^n_{L/R} = \mathcal{M}_n^2\psi^n_{L/R}. \tag{3.81}$$

If we plug in a confining harmonic potential

$$\varphi(z) = \kappa^2 z^2, \tag{3.82}$$

we find

$$\left[-\partial_z^2 + \kappa^4 z^2 + 2\kappa^2\left(\mu R \mp \frac{1}{2}\right) + \frac{\mu R\,(\mu R \pm 1)}{z^2}\right]\psi^n_{L/R} = \mathcal{M}^2_{L/R}\psi^n_{L/R}, \tag{3.83}$$

with the normalisation

$$\int_0^\infty \mathrm{d}z\psi^m_{L/R}\psi^n_{L/R} = \delta^{mn}. \tag{3.84}$$

On should also note, that for $d = 4$ and $\tau = 3 + L$, the effective mass $\mu R = L + 3/2$.

The Light-Front Baryons

In physical LF space-time, spin-1/2 particles obey the Dirac equation

$$D_{LF}\,|\psi\rangle = \mathcal{M}\,|\psi\rangle\,, \tag{3.85}$$

where D_{LF} is a Hermitian operator. Using integrability methods [49, 50], any equation of motion of a physical state can be factorised in terms of ladder operators generating all eigenfunctions from the lowest eigenfunction. Rather than formally deriving the Dirac operator from first principles, the Dirac operator is now expressed in terms of the matrix-valued non-hermitian operator Π:

$$\begin{aligned} D_{LF} &= \alpha\Pi, \quad \text{with} && (3.86)\\ \Pi_\nu &= -i\left(\frac{\mathrm{d}}{\mathrm{d}\zeta} - \frac{\nu+1/2}{\zeta}\gamma_5 + i\kappa^2\zeta\gamma_5\right) && (3.87) \end{aligned}$$

in the soft-wall case [51]. In the hard-wall scenario, one discards the κ-dependent terms. α is an anti-commuting 4×4 hermitian matrix with $\alpha^2 = 1$.

Because of the hermiticity of D_{LF}, $D_{LF}^2 = \mathcal{M}^2 = H_{LF}$, and thus we can write

$$\begin{aligned} H_{LF}^{\nu} &= \Pi_\nu^\dagger\Pi_\nu + C \\ &= -\frac{\mathrm{d}^2}{\mathrm{d}\zeta^2} + \frac{(\nu+1/2)^2}{\zeta^2} - \frac{\nu+1/2}{\zeta^2}\gamma_5 \\ &\quad +\kappa^4\zeta^2 + \kappa^2(2\nu+1) + \kappa^2\gamma_5, \end{aligned} \tag{3.88}$$

where a constant C is chosen to be zero for the time being. We find the equations of motion in the light-front to be

$$\begin{aligned} \left(-\frac{\mathrm{d}^2}{\mathrm{d}\zeta^2} - \frac{1-4\nu^2}{4\zeta^2} + \kappa^4\zeta^2 + 2(\nu+1)\kappa^2\right)\psi_R &= \mathcal{M}_R^2\psi_R && (3.89)\\ \left(-\frac{\mathrm{d}^2}{\mathrm{d}\zeta^2} - \frac{1-4(\nu+1)^2}{4\zeta^2} + \kappa^4\zeta^2 + 2\kappa^2\nu\right)\psi_L &= \mathcal{M}_L^2\psi_L. && (3.90) \end{aligned}$$

These equations differ from the ones presented in reference [35] a bit. We will from here on adopt the notation used there, and call $\psi_R \equiv \psi_+$ and $\psi_L \equiv \psi_-$.

The Equations (3.89) and (3.90) can be mapped to the Equations (3.83) by reusing $\zeta = z$ and choosing ν as

$$\nu = |\mu R| - \frac{1}{2} = L + 1. \tag{3.91}$$

The Hermicity of the Dirac operator D_{LF} implies that for a hard-wall model, the surface term $\psi_+^*\psi_- - \psi_-^*\psi_+$ should vanish at the boundaries. This implies that either ψ_+ or ψ_- should vanish at the boundaries $\zeta = 0$ and $\zeta = \zeta_0$.

The extension of this formalism to spin-3/2 and higher spins is straightforward. However, the detailed discussion of this extension is not strictly relevant for the goal of this thesis.

3.4 Hard- and Soft-Wall Models for Hadrons

There are two different ways to truncate the AdS space that present two alternative AdS/QCD backgrounds:

1. the hard-wall IR brane cut-off
2. the soft-wall method by
   (a) a dilaton background field
   (b) warping of the AdS metric
   (c) incorporating a cut-off to $U(z)$

of which the three soft-wall methods are equivalent [48]. Also, a *no-wall* holographic model has been proposed, motivated by the soft-wall method, but with the dilaton prefactor moved to the effective potential by a dilaton transformation, where the dilaton field is then replaced by a dilaton condensate. [48]

In this thesis, the dilaton background has been introduced into the effective actions (3.34) and (3.71) without any consideration. The exponential metric modification can be seen as a gravitational potential $V(z) = m\sqrt{g_{00}} = \frac{mR}{z}\exp(\pm 3\varphi/4)$ in the fifth dimension of AdS. The negative solutions make the potential decrease monotonically, and so an object will always fall to infinitely large values of z. Positive solutions result in the potential having

an absolute minimum at $z \sim \kappa^{-1}$ and it increases exponentially, effectively confining the objects under consideration around the minimum. [35]

There is a lot of discussion in the literature about the sign of the dilaton profile $\exp(\pm\varphi(z))$. For instance, references [48, 52] argue for the negative sign producing the correct Regge-like behaviour of the meson spectrum and claim that a positive sign produces a spurious massless scalar mode of the vector channel and has extra potential terms. However, [35] argue that the difference between the two signs is merely a z-independent shift $\Delta U = 4(J-1)\kappa^2$ in the effective potential for $\varphi = \pm\kappa^2 z^2$. Here, the positive sign is chosen.

If we want the pion $\pi(140)$ to be massless in the chiral limit, we find that the confining potential (3.52) is unique – with the dilaton $\varphi(z) \propto z^s$ we find that only $s = 2$ fulfils the condition [34, 53].

Even if the hard-wall method is the pedagogically easier approach on the subject, it has its pitfalls. It cannot account for a_1,a_2,a_3 triplet splitting, $I \neq 1$ mesons are too complex for the model, $n > 0$ excitations have too large masses, $\mathcal{M}_{\pi(140)} \neq 0$, and more importantly it produces a mass spectrum $\mathcal{M} = \beta_{L,k}\Lambda_{\mathrm{QCD}} \sim 2n + L$, not the hoped for $\mathcal{M}^2 \sim n + L$ Regge behaviour [35]. Therefore we will focus solely on the soft-wall model.

3.4.1 Meson Masses

To achieve confinement, let us take the dilaton profile to be

$$\varphi(\zeta) = \kappa^2\zeta^2, \tag{3.92}$$

and by using Equation (3.52), we have a confining potential

$$U(\zeta) = \kappa^4\zeta^4 + 2\kappa^2(J-1). \tag{3.93}$$

The normalisation is

$$\int_0^\infty \mathrm{d}\zeta \phi_J^2(\zeta) = 1. \tag{3.94}$$

Now, Equation (3.51) is

$$\left(-\frac{\mathrm{d}^2}{\mathrm{d}\zeta^2} - \frac{1-4L^2}{4\zeta^2} + \kappa^4\zeta^4 + 2\kappa^2(J-1)\right)\phi_J(\zeta) = \mathcal{M}^2\phi_J(\zeta). \tag{3.95}$$

A change of variables to $u = \kappa\zeta$ allows us to rewrite this as

$$\left(-\frac{\mathrm{d}^2}{\mathrm{d}u^2} + \frac{4L^2-1}{4u^2} + u^2 + 2(J-1)\right)\kappa^2\phi_J(u) = \mathcal{M}^2\phi_J(u), \tag{3.96}$$

which is solved by a substitution

$$\phi_J(u) = u^{L+1/2}\mathrm{e}^{-u^2/2}\psi(u). \tag{3.97}$$

This results in the Laguerre equation

$$u^2\frac{\mathrm{d}^2\psi}{\mathrm{d}u^2} + (1-u^2)\frac{\mathrm{d}\psi}{\mathrm{d}u} + nu^2\psi = -L\frac{\mathrm{d}\psi}{\mathrm{d}u}, \tag{3.98}$$

where the eigenvalue $\mathcal{M}^2$ has been already plugged in for clarity,

$$\mathcal{M}^2 = 4\kappa^2\left(n + \frac{J+L}{2}\right). \tag{3.99}$$

The solutions of equation (3.98) are

$$\psi_n^L(\zeta) = CL_n^L(\kappa^2\zeta^2), \tag{3.100}$$

where C is a normalisation constant and L_n^L is a Laguerre polynomial. Using the result

$$\int_0^\infty \mathrm{d}x\; x^L e^{-x} L_n^L(x)^2 = \frac{\Gamma(n+L+1)}{n!}, \tag{3.101}$$

the normalisation (3.94) with (3.97) yields

$$\phi_{n,L}(\zeta) = \kappa^{1+L}\sqrt{\frac{2n!}{(n+L)!}}\zeta^{L+1/2}\mathrm{e}^{-\kappa^2\zeta^2/2}L_n^L(\kappa^2\zeta^2). \tag{3.102}$$

Unlike the hard-wall model, the soft-wall model accounts well for the triplet splitting of $a_0(980)$, $a_1(1260)$ and $a_2(1320)$, with respective masses of 0.98, 1.23 and 1.32 GeV; Equation (3.99) gives us the predictions of 0.76, 1.08 and 1.32 GeV for $\kappa = 0.54$. Also, the lowest excitation of the pion $\pi(140)$ has the quantum numbers $n = L = J = 0$, thus giving the expected $\mathcal{M}^2 = 0$ from Equation (3.99).

The soft-wall model also is less ambiguous than the hard-wall model, as we need not choose any boundary conditions for the LFWFs. Though, one needs to fix the constant Λ_{QCD} or κ in both models, therefore choosing a fitting cut-off for the theory *ad hoc*.

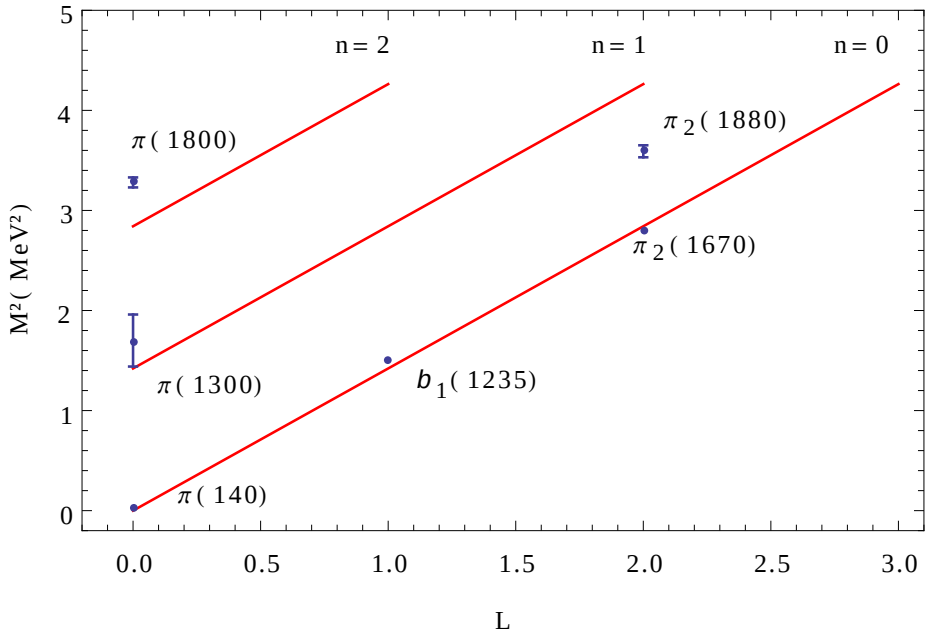

Figure 3.5: The best fit of (3.95) for pseudoscalar mesons in the soft-wall model with $\kappa = 0.60\text{GeV}$.

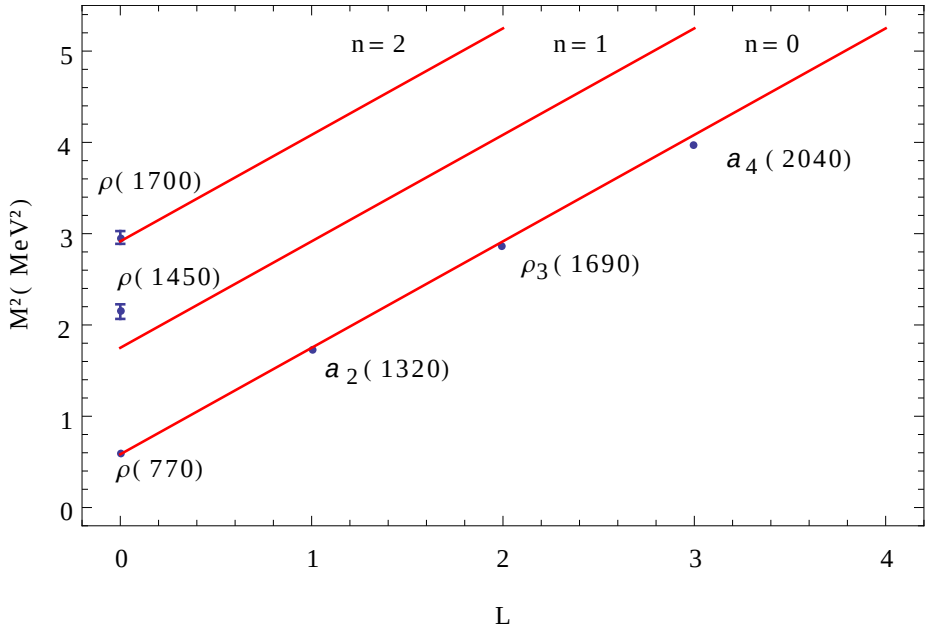

Figure 3.6: The best fit of (3.95) for vector mesons in the soft-wall model with $\kappa = 0.54\text{GeV}$.

3.4.2 Baryon Masses

When solving equations (3.89) and (3.90), we can make use of the similarities with the meson case (3.95), and notice the baryon equations also point to the Laguerre equation with the eigenvalues

$$\mathcal{M}^2 = 4\kappa^2(n+\nu+1), \tag{3.103}$$

$$\tag{3.104}$$

for both chiralities for $\kappa^2 > 0$. There exists no solutions for $\kappa^2 < 0$ [39]. The eigenfunctions are

$$\psi_+(\zeta) \sim \zeta^{\nu+1/2} \mathrm{e}^{-\kappa^2\zeta^2/2} L_n^{\nu}(\kappa^2\zeta^2), \tag{3.105}$$

$$\psi_-(\zeta) \sim \zeta^{\nu+3/2} \mathrm{e}^{-\kappa^2\zeta^2/2} L_n^{\nu+1}(\kappa^2\zeta^2). \tag{3.106}$$

As we want to ensure the universality of the Regge slope for both mesons and baryons, we should use a similar κ for both mesons and baryons. This is necessary, as the redefinition of the fields scales the dilaton away and leaves us without a specified energy scale. To ensure the mass scales of the light-front models for both mesons and baryons are equal, we need to subtract $4\kappa^2$ from Equation (3.103), effectively choosing $\nu = L$. [35, 54] This has one problem, as now the lowest energy state $n = L = 0$ actually corresponds to a twist-2 trajectory instead of the wanted twist-3, the twist corresponding to the number of partons inside the hadron [42]. This is noteworthy, as the scaling behaviour with $\tau = 3$ corresponds to one of an $N_C = 3$ baryon, not the usual $N_C \to \infty$ solitons or Skyrmion-like objects found in top-down approaches [35, 55, 56].

One needs to do some other phenomenological tweaks to the mass term in order to ensure the agreement with the experiments. The mass is expected to increase similarly as with the mesons when the radial quantum number n. Internal orbital angular momentum L and the internal spin S are increased with 1 unit, thus giving us the gaps $\Delta n = 4\kappa^2$, $\Delta L = 4\kappa^2$ and $\Delta S = 2\kappa^2$, leaving us with

$$\mathcal{M}^2_{n,L,S} = 4\kappa^2 \left(n + L + \frac{S}{2} + \frac{3}{4} \right). \tag{3.107}$$

Also, in Nature, baryons with the same n, L and S, but different parities, do have different masses, unlike what one would expect from the eigenvalues

(3.103). We can achieve this difference by choosing the branch $\nu = \mu R - 1/2$ for negative-parity baryons with $S = 3/2$. [35] Doing the same procedure for the new-found negative-parity mass as we did for the positive-parity mass, we end up with the masses

$$\mathcal{M}^{2(+)}_{n,L,S} = 4\kappa^2 \left(n + L + \frac{S}{2} + \frac{3}{4} \right), \tag{3.108}$$

$$\mathcal{M}^{2(-)}_{n,L,S} = 4\kappa^2 \left(n + L + \frac{S}{2} + \frac{5}{4} \right). \tag{3.109}$$

These are fitted to the confirmed 3- and 4-star nucleons and Δ baryons in Figures 3.7, 3.8 and 3.9 respectively. The masses and the quantum numbers of the baryons are catalogued in Tables A.3 and A.4 in Appendix A.

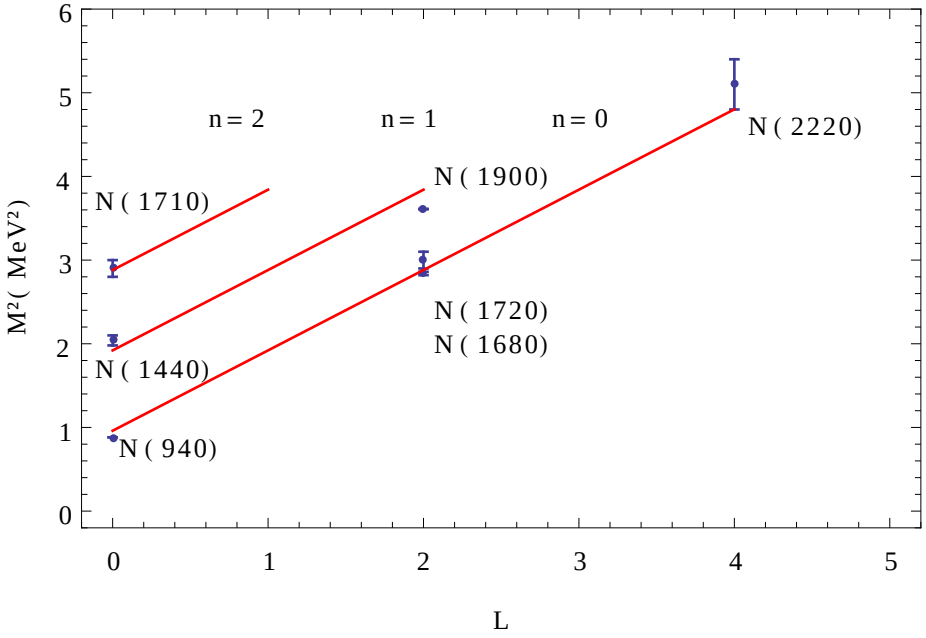

Figure 3.7: The positive parity nucleon resonances fitted with Equation (3.108) for $\kappa = 0.49$GeV.

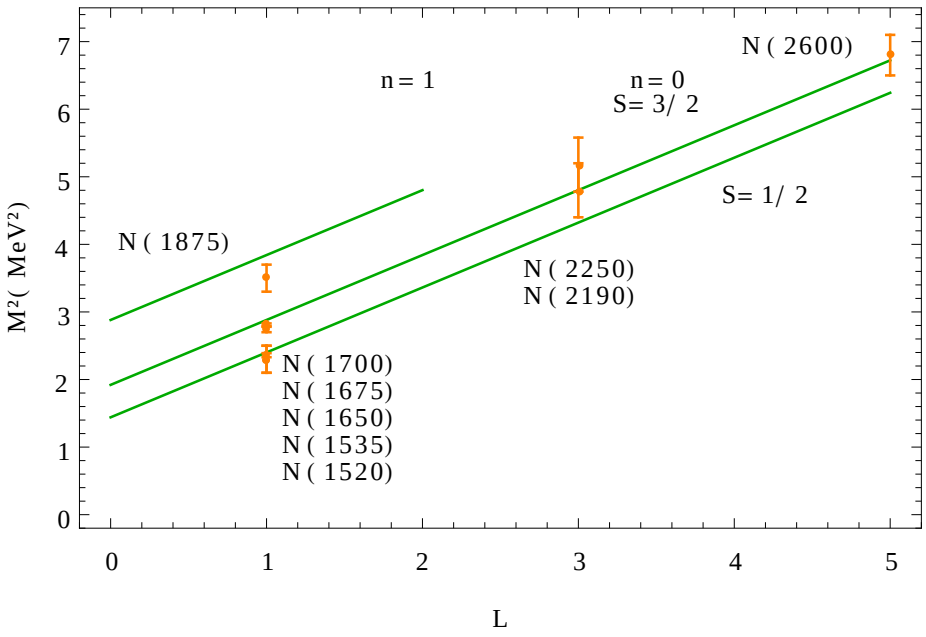

Figure 3.8: The negative parity nucleon resonances fitted with Equation (3.109) for $\kappa = 0.49\text{GeV}$.

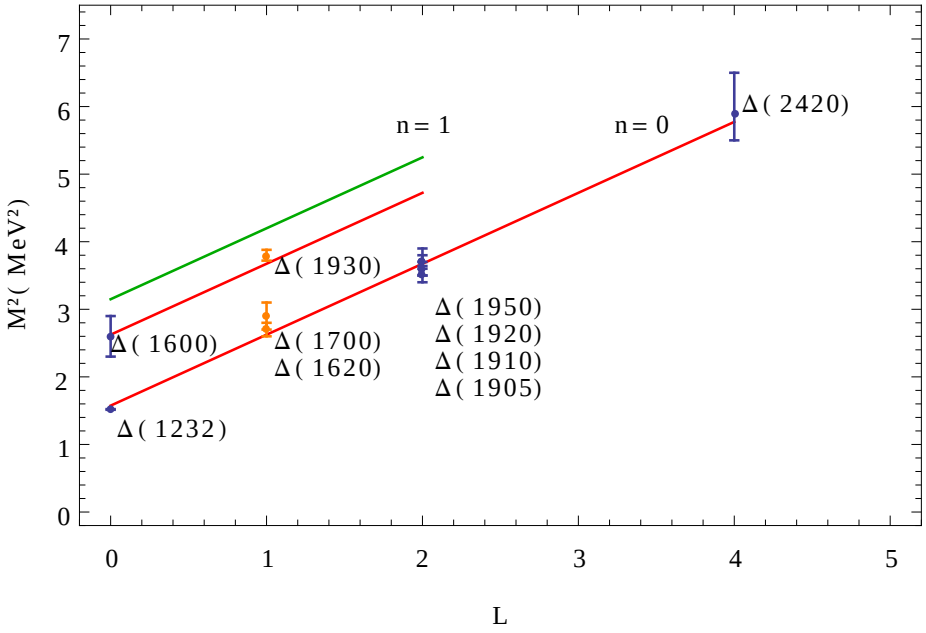

Figure 3.9: Positive (blue dots) and negative (orange dots) parity Delta resonances fitted with Equations (3.109) (green line) (3.108) (red lines) for $\kappa = 0.51\text{GeV}$. All the positive parity Deltas have spin 3/2 and, of the negative parity resonances, only the $n = 1$ excitation $\Delta(1930)$ has spin 3/2. Therefore the $n = 0$ slope is the same for both the negative and positive parity Deltas.

As with the mesons, the soft-wall model is successful in reproducing the correct Regge slopes, even if more phenomenological tinkering is needed to improve the fit. Still, the radial excitations $n > 0$ are all well accounted for and parity degeneracy of the light baryon spectrum is included, like the pair $N(1680)$ and $N(1720)$ at $L = 2$.

The cluster decomposition of the ζ for arbitrary n,

$$\zeta = \sqrt{\frac{x}{1-x}} \left| \sum_{j=1}^{n-1} x_j \mathbf{b}_{\perp j} \right|, \tag{3.110}$$

can be seen as a quark-diquark model for baryons with $n = 3$ quarks, where one has one active quark with momentum fraction x and two observers with momentum fraction $1 - x$.

One important thing to note is that the LFWFs (3.105) and (3.106) are not independent – they must also obey the linear Dirac equation and therefore the relative normalisation is fixed. Thus the different parities have equal probability

$$\int \mathrm{d}\zeta \psi_+^2(\zeta) = \int \mathrm{d}\zeta \psi_-^2(\zeta) = 1. \tag{3.111}$$

This implies that spin of the partons in the baryon have equal probability to be aligned or anti-aligned with proton spin J^z. Thus the states $L_q^z = 0$ and $L_q^z = \pm 1$ have equal probabilities. Therefore proton spin is completely carried by the angular momentum of quarks $J^z = \langle L_q^z \rangle = \pm 1/2$ at the chiral limit.

3.5 Form Factors for Hadrons

As the late Richard Feynman once said: "One very powerful way of experimentally investigating the strongly interacting particles (hadrons) is to look at them" [57]. Form factors do exactly this: they describe in a compact manner how a hadron interacts with a photon.

The form factors in QCD are transition matrix elements of a local quark current $J^\mu = \sum_q e_q \bar{q} \gamma^\mu q$ between two different hadronic states $|P'\rangle = |P + q\rangle$ and $|P\rangle$ [35, 39]. They describe the distributions of electric charge and current inside a hadron, and are thus important when studying the inner workings of hadrons. [58]

In instant-form the form factors are heavily frame-dependent and just knowing the wave function of a particle is not sufficient to determine the hadronic properties, as one also needs to include the vacuum processes. Calculating the matrix elements $\langle P+q|J^\mu(0)|P\rangle$ requires a boost from $|P\rangle$ to $|P+q\rangle$, which is a considerable complication, as even the particle number changes in the boosted frame [59].

On the other hand, the light-front wave functions are boost-invariant and contain all the physical information needed, and the boost operators do not have interaction terms. The space-like form factors can be represented as overlap integrals of the Fock state wave functions using the Drell-Yan-West (DYW) formula [44, 45]. [32]

3.5.1 Meson Form Factors

The electromagnetic current has elementary couplings to the constituent quarks, and in the interaction picture the full Heisenberg current can be expressed by the free quark current $J^\mu(0)$ at fixed light-cone time $x^+ = 0$ in the $q^+ = 0$ frame.

So, in physical space-time one can define the form factor as the transition matrix element of the quark current between two hadronic states

$$\langle P'|J^\mu(0)|P\rangle = (P+P')^\mu F_M(q^2), \tag{3.112}$$

where $J^\mu = \sum_q e_q \bar{q}\gamma^\mu q$.

To avoid coupling to Fock states with different numbers of constituents, the form factor in the light-front is computed from the plus-component $J^+ = \sum_q e_q \bar{q}\gamma^+ q$ of the current, because the γ^+ conserves the spin component of the struck quark [35, 39].

Now, expanding the states $|P\rangle = |\psi_M(P^+, \mathbf{P}_\perp\rangle$ in their Fock components $\psi_n(x_j, \mathbf{b}_{\perp_j}, \lambda_j)\,|n\rangle$ and integration in the $q^+ = 0$ frame, one finds the DYW formula [51, 60]

$$F_M(q^2) = \sum_n \int \mathrm{d}[x_j][\,\mathrm{d}^2\mathbf{k}_{\perp j}] \sum_j e_j \psi_n^*(x_j, \mathbf{k}'_{\perp j})\psi_n(x_j, \mathbf{k}_{\perp j}), \tag{3.113}$$

where the integrals $[\,\mathrm{d}x_i]$ and $[\,\mathrm{d}^2\mathbf{k}_{\perp j}]$ are given by Equations (3.24), and $\mathbf{k}'_{\perp j} = \mathbf{k}_{\perp j} + (1-x_j)\mathbf{q}$ for every struck constituent and $\mathbf{k}'_{\perp j} = \mathbf{k}_{\perp j} - x_j\mathbf{q}$ for every spectator constituent with the photon having had momentum $\mathbf{q}$.

This can be further simplified by using the conjugate variable of $\mathbf{k}_\perp$; $\mathbf{b}_\perp$, as the previous equation is then expressible only in terms of the spectator constituents [39, 60]

$$F_M(q^2) = \sum_n \prod_{j=1}^{n-1} \int \mathrm{d}x_j \, \mathrm{d}^2\mathbf{b}_{\perp j} \exp\left[i\mathbf{q}_\perp \cdot \sum_{k=1}^{n-1} x_k \mathbf{b}_{\perp k} \right] |\psi_n(x_j, \mathbf{b}_{\perp j})|^2 , \quad (3.114)$$

as the integration over $\mathbf{k}_\perp$ space gives $n-1$ delta functions.

As long as one sums over all the Fock components – the infinite lot – the formula (3.114) is an exact expression of the form factor.

In the gravity theory in AdS space the form factors are overlap integrals of the normalisable modes propagating in AdS space with boundary currents propagating in bulk [35]. Given a (spinless, in this case) wave function $\Phi_P(x,z)$ describing a meson with momentum P in the AdS space coupling non-locally to an external electromagnetic field $A^M(x,z)$ with polarisation along the physical indices, one can write the Polchinski-Strassler formula [43] for the form factor $F(q^2)$ [51]

$$\int \mathrm{d}^4x \, \mathrm{d}z \; e_5 \sqrt{g} A^M \Phi^*_{P'} \overleftrightarrow{\partial_M} \Phi_P \sim (2\pi)^4 \delta^{(4)}(P' - P - q) \epsilon_\mu (P + P')^\mu e F(q^2), \quad (3.115)$$

where $q = P' - P$ is the four-momentum of the photon, ϵ_μ is its polarisation vector, e_5 is the 5 dimensional coupling to the electromagnetic field and e is the physical coupling to the electromagnetic field in the light-front and $\alpha \overleftrightarrow{\partial_M} \beta = (\partial_M \alpha)\beta - \alpha \partial_M \beta$. The left-hand side of the equation is simply the interaction term of the AdS_5 action. The form of the derivative is due to the covariant derivative $D_M = \partial_M - ieA_M$, the interactions coming from the cross terms of the product $(D_M \Phi^*)(D^M \Phi)$.

Free Current

To explore the possibilities of the duality, let us start from the simplest case of a free current propagating in AdS_5 and then move to confine the current to fit the previously discussed hard- and soft-wall models.

The equations of motion for the external photon field A^M in AdS are extracted from the action

$$S_{EM} = \int \mathrm{d}^4x \, \mathrm{d}z \sqrt{g} g^{MM'} g^{NN'} F_{MN} F_{M'N'}, \quad (3.116)$$

where the covariant field tensor is $F_{MN} = \partial_M A_N - \partial_N A_M$. If we substitute

$$A_\mu = \mathrm{e}^{iq\cdot x} V(q^2, z)\epsilon_\mu(q), \tag{3.117}$$

$$A_z = 0, \tag{3.118}$$

where $V(q^2, z)$ is the bulk-to-boundary propagator, we can write the EOM as

$$\left[\frac{\mathrm{d}^2}{\mathrm{d}z^2} - \frac{1}{z}\frac{\mathrm{d}}{\mathrm{d}z} - Q^2\right] V(Q^2, z) = 0, \tag{3.119}$$

where $Q^2 = -q^2 > 0$. The boundary conditions for the bulk-to-boundary propagator are

$$V(q^2 = 0, z) = V(q^2, z = 0) = 1. \tag{3.120}$$

This is because the propagator should have a value of 1 at zero momentum transfer as the bulk solution should be normalised to the total charge operator, and at $z = 0$ the external current is $A^M(x^\mu, 0) = e^{iq\cdot x}\epsilon_\mu(q)$ [53, 54].

With the boundary conditions (3.120), and substitutions $\alpha = zQ$ and $\tilde{V} = \alpha V$, the solutions to Equation (3.119) are

$$V(Q^2) = zQK_1(zQ), \tag{3.121}$$

where K_1 is the modified Bessel function of the first kind.

After integration over the Minkowski coordinates, the Equation (3.115) can be written as

$$F(q^2) = R^3 \int_0^{\Lambda_{\mathrm{QCD}}^{-1}} \frac{\mathrm{d}z}{z^3} V(q^2, z)\Phi^2(z). \tag{3.122}$$

The expansion of the previous expression to the spin-J mesons can be done by rescaling [39]

$$\Phi_J(z) = \left(\frac{z}{R}\right)^J \Phi(z). \tag{3.123}$$

The modified Bessel function times its argument $zQK_1(zQ) = V(zQ)$ has an integral representation [35]

$$V(zQ) = \int_0^1 \mathrm{d}x J_0\left(zQ\sqrt{\frac{1-x}{x}}\right), \tag{3.124}$$

and so the electromagnetic form factor (3.122) can be written as

$$F(q^2) = R^3 \int_0^1 \mathrm{d}x \int \frac{\mathrm{d}z}{z^3} J_0 \left(zQ\sqrt{\frac{1-x}{x}} \right) \Phi^2(z). \tag{3.125}$$

The identification of the duality between the AdS_5 gravity theory and light-front QCD can now be made in a simple case of π^+ valence Fock state $|u\bar{d}\rangle$. The light-front form factor for the aforementioned state is acquired from Equation (3.114) by integrating over angles, exchanging $x \leftrightarrow 1-x$ and using the integral representation of J_0,

$$J_0(x) = \frac{1}{2\pi} \int_0^{2\pi} \mathrm{e}^{ix\cos(t)}\, \mathrm{d}t. \tag{3.126}$$

One finds

$$F_{\pi^+} = 2\pi \int_0^1 \frac{\mathrm{d}x}{x(1-x)} \int \zeta\, \mathrm{d}\zeta J_0 \left(zQ\sqrt{\frac{1-x}{x}} \right) |\psi_{u\bar{d}}(x,\zeta)|^2, \tag{3.127}$$

where $\zeta^2 = x(1-x)\mathbf{b}_\perp^2$, $e_u = 2/3$ and $e_{\bar{d}} = 1/3$.

The expressions (3.127) and (3.125) can be mapped to each other after we use the expression

$$\psi(x,\zeta,\theta) = \mathrm{e}^{iL\theta} X(x) \frac{\phi(\zeta)}{\sqrt{2\pi\zeta}}, \tag{3.128}$$

for the LFWF. Assuming that both form factors agree for arbitrary Q, the mapping is found to be

$$\phi(\zeta) = \left(\frac{R}{\zeta} \right)^{-3/2} \Phi(\zeta), \tag{3.129}$$

$$X(x) = \sqrt{x(1-x)}. \tag{3.130}$$

One can map the DYW formula (3.114) to the gravity theory on AdS state-by-state, but this proves to have some problems. For example, the multipole structure of the time-like form factor does not appear before one has included an infinite number of LF Fock components, and on the $Q^2 \to 0$ limit the charge radius goes to infinity, as the momenta diverge.

Hard-Wall Model with Confined Current

Setting a hard-wall boundary condition for the current in the $z_0 = \Lambda_{\mathrm{QCD}}^{-1}$ limit confines it to the IR modified AdS space. The boundary condition $A(z) = 0$ leads to [61]

$$V(Q^2, z) = zQ\left[K_1(zQ) + \frac{K_0(Q/\Lambda_{\mathrm{QCD}})}{I_0(Q/\Lambda_{\mathrm{QCD}})} I_1(zQ)\right]. \tag{3.131}$$

The expression has an infinite series of time-like poles at the zeroes of the modified Bessel function $I_0(Q/\Lambda_{\mathrm{QCD}})$, which is what one should expect, because $I_\alpha(x) = e^{-i\alpha\pi/2} J_\alpha(ix)$, thus corresponding to the zeroes of the $L = 0$, $\tau = 2$ solutions for the mesonic LFWE. So, the poles in the current are determined by the mass spectrum of radial excitations of mesons in the hard-wall model. [39]

The hard-wall model is thus self-consistent, but the mass spectrum is still asymptotically $\mathcal{M} \sim 2n$ instead of the Regge trajectory $\mathcal{M}^2 \sim n$ for $L = 0$, which places the time-like poles of the form factor to an incorrect position.

Soft-Wall Model

For the soft-wall model, the effective potentials (3.115) and (3.116) need to be multiplied by the usual exponential dilaton background and the 5-dimensional effective coupling $e_5(z)$ should be taken to be z-dependent. We end up with the AdS form factor

$$eF(Q^2) = R^3 \int \frac{\mathrm{d}z}{z^3} \mathrm{e}^{\varphi(z)} e_5(z) V(Q^2, z) \Phi^2(z). \tag{3.132}$$

The equation of motion for the bulk-to-boundary propagator is now

$$\left[\frac{\mathrm{d}^2}{\mathrm{d}z^2} - (z^{-1} - \varphi'(z))\frac{\mathrm{d}}{\mathrm{d}z} - Q^2\right] V(Q^2, z) = 0, \tag{3.133}$$

with the boundary conditions

$$\lim_{Q\to 0} \frac{e_5(z)}{e} V(Q^2, z) = \lim_{z\to 0} \frac{e_5(z)}{e} V(Q^2, z) = 1. \tag{3.134}$$

The solution to Equation (3.133) for the dilaton profile $\varphi = \kappa^2 z^2$, with $\kappa^2 > 0$ is

$$V(Q^2, z) = \mathrm{e}^{-\kappa^2 z^2} \Gamma\left(1 + \frac{Q^2}{4\kappa^2}\right) U\left(\frac{Q^2}{4\kappa^2}, 0, \kappa^2 z^2\right), \tag{3.135}$$

where

$$U(a,b,c) = \frac{1}{\Gamma(a)} \int_0^\infty \mathrm{d}t\ \mathrm{e}^{-ct} t^{a-1} (1+t)^{b-a-1} \tag{3.136}$$

is the Tricomi confluent hypergeometric function.

From the boundary conditions (3.134) we get

$$e_5(z) = e\mathrm{e}^{k^2 z^2}, \tag{3.137}$$

assuming $\kappa^2 > 0$. The fact that the 5 dimensional coupling is z-dependent does not affect the gauge symmetries in the lower-dimensional physical space-time, as the functional dependence is determined by the boundary conditions ensuring charge conservation in Minkowski space at $Q^2 = 0$. [39]

Using the integral representation of the Tricomi hypergeometric function we find for a modified propagator $\tilde{V}(Q^2, z) = \dfrac{e_5(z)}{e} V(Q^2, z)$ [39],

$$\tilde{V}(Q^2, z) \;=\; \kappa^2 z^2 \int \frac{\mathrm{d}x}{(1-x)^2} x^{Q^2/4\kappa^2} \mathrm{e}^{-\kappa^2 z^2 x/(1-x)}. \tag{3.138}$$

To see the pole-structure of (3.138), let us alter it a bit. Using the relation [62]

$$\sum_{n=0}^{\infty} L_n^k(z) x^n = \frac{\mathrm{e}^{-zx/(1-x)}}{(1-x)^{k+1}} \tag{3.139}$$

for associated Laguerre polynomials $L_n^k(z)$, we obtain

$$\begin{aligned} \tilde{V}(Q^2, z) &= \sum_{n=0}^{\infty} \kappa^2 z^2 L_n^1(\kappa^2 z^2) \int \mathrm{d}x\ x^{Q^2/4\kappa^2} x^n \\ &= \sum_n \frac{4\kappa^4 z^2 L_n^1(\kappa^2 z^2)}{Q^2 + 4\kappa^2 (n+1)}. \end{aligned} \tag{3.140}$$

For a meson with $n = 0$, $L = 0$ and arbitrary twist τ described by hadronic state

$$\Phi_\tau(z) = \sqrt{\frac{2}{\Gamma(\tau - 1)}} \kappa^{\tau - 1} z^\tau \mathrm{e}^{-\kappa^2 z^2/2}, \tag{3.141}$$

where the dilaton is absorbed in the wave function for convenience, the form factor is (using the (3.138) form of the propagator)

$$\begin{aligned} F_\tau(Q^2) &= \int_0^1 \mathrm{d}x\ (\tau - 1)(1-x)^{\tau - 2} x^{Q^2/4\kappa^2} \\ &= \Gamma(\tau) \frac{\Gamma\left(1 + \frac{Q^2}{4\kappa^2}\right)}{\Gamma\left(\tau + \frac{Q^2}{4\kappa^2}\right)}. \end{aligned} \tag{3.142}$$

Using a recurrence relation $\Gamma(n+z) = (n-1+z)(n-2+z)\cdots(1+z)\Gamma(1+z)$ and assuming integer τ, the form factor can be expressed as

$$F_\tau = \frac{1}{\left(1+\frac{Q^2}{4\kappa^2(\tau-1)}\right)\left(1+\frac{Q^2}{4\kappa^2(\tau-2)}\right)\cdots\left(1+\frac{Q^2}{4\kappa^2}\right)}, \tag{3.143}$$

which has $\tau - 1$ time-like poles along the Regge trajectory.

The time-like poles of (3.143) occur at $-Q^2 = \mathcal{M}_\rho^2 = 4\kappa^2(n+1)$, which should be the masses of $J = 1, L = 0$ vector mesons. In actuality, in the soft-wall model, their mass eigenvalues are given by Equation (3.99) to be $\mathcal{M}^2 = 4\kappa^2(n+1/2)$, so we shift the masses in Equation (3.143) to match their $\tau = 2$ mass poles of the model and to give better agreement with the measurements.

Further phenomenological modifications arise when one considers the resonance widths of the hadrons. The hadrons are stable and have zero width in the strongly coupled semiclassical gauge/gravity duality, but in reality the resonances have a width [53]. So, it is a reasonable phenomenological modification of the light-front holographic pion form factor to include the widths in the expressions as [39, 63]

$$F_\tau(q^2) = \frac{\mathcal{M}_\rho^2\mathcal{M}_{\rho'}^2\cdots\mathcal{M}_{\rho^{\tau-2}}^2}{(\mathcal{M}_\rho^2 - q^2 - iq\Gamma_\rho)(\mathcal{M}_{\rho'}^2 - q^2 - iq\Gamma_{\rho'})\cdots((\mathcal{M}_{\rho^{\tau-2}}^2 - q^2 - iq\Gamma_{\rho^{\tau-2}})}, \tag{3.144}$$

where $\mathcal{M}_{\rho^\tau}$ is the mass of the τ^{th} resonance of ρ, and Γ_τ is its corresponding width.

In general, hadrons should be considered as a superposition of an infinite number of Fock states, and thus the individual form factors are not the whole truth. The full pion form factor can be acquired by summing an infinite number of twist-τ states

$$F_\pi(q^2) = \sum_\tau P_\tau F_\tau, \tag{3.145}$$

where P_τ is the probability of finding the particle in a twist-τ state (so $\sum_\tau P_\tau = 1$).

In Figure 3.10 the elastic form factor (3.144) has been computed in the low momentum transfer regime in a truncated form: only twist-2 and twist-4

terms are included in the calculation with probabilities $P_{\tau=4} = 12.5\%$ and $P_{\tau=2} = 87.6\%$, i.e.

$$F_\pi(q^2) \approx (1 - P_{\tau=4})F_{\tau=2}(q^2) + P_{\tau=4}F_{\tau=4}(q^2). \tag{3.146}$$

The chosen widths do agree with [28], even as they are on the lower side. The probabilities of the states are an input for the model.

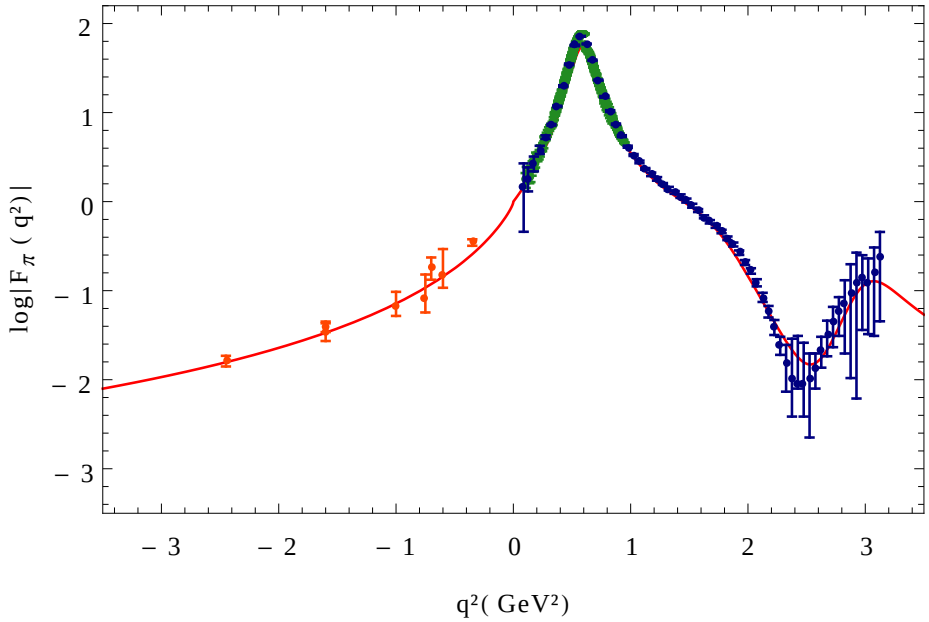

Figure 3.10: The space-like ($q^2 < 0$) and time-like ($q^2 > \mathcal{M}_\rho^2$), $\tau = 4$ truncated pion elastic form factor $\log|F_\pi(q^2)|$ at low momentum transfer for $\kappa = 0.5482$ GeV, $P_{\tau=4} = 12,5\%$ and widths of ρ resonances chosen to be $\Gamma_\rho = 149$ MeV, $\Gamma_{\rho'} = 460$ MeV and $\Gamma_{\rho''} = 160$ MeV. The time-like results are by Belle (blue dots) [64] and by KLOE collaboration (green dots) [65–67], and the space-like results are by JLAB FPi collaboration (orange dots) [68–70] .

It is clear that the effective semiclassical light-front holographic model for the pion form factor is in quite a good agreement with the experimental results, even if the model is a crude one. In the higher-energy regime the model however falls short [71], and interference with higher twist modes, the q^2-dependence of the resonance widths and mixing with the continuum should be incorporated to the model to improve the accuracy at higher energies. If the transferred time-like momenta is large enough, the resonance structure should be less important, as then the $\tau = 2$ term dominates in (3.144). [39]

Effective Light-Front Wave Function from the Mapping of the Current

As a side note, one can also find the LFWFs via the holographic mapping of the EM current propagating in the gravity realm to the LFQCD DYW expression. Then one would find an effective wave function, which corresponds to a superposition of an infinite number of Fock states, as the current was not truncated at any point, unlike the straight-on computation of the LFWFs.

The effective wave function can be most easily deduced by the fact, that the form factor can be written as [60]

$$F(Q^2) = \int_0^1 \mathrm{d}x \rho(x, Q), \tag{3.147}$$

in terms of the single-particle density. For a two-parton state the density can be written

$$\rho(x, Q) = 2\pi \int_0^\infty b \, \mathrm{d}b J_0(bQ(1-x))|\psi(x, b)|^2, \tag{3.148}$$

and thus one can deduce the effective two-parton wave function to be [72]

$$\psi_{\text{eff}}(x, \mathbf{b}_\perp) = \kappa \frac{1-x}{\sqrt{\pi \log(x^{-1})}} \exp\left[-\frac{\kappa^2 \mathbf{b}_\perp^2 (1-x)^2}{2 \log(x^{-1})}\right]. \tag{3.149}$$

This wave function encodes aspects of the LFQCD that cannot be determined from a finite number of terms of term-by-term holographic mapping. It is not symmetrical in the longitudinal variables x and $1-x$ for the active and spectator quarks, but it still has the correct analytical properties [39].

3.5.2 Nucleon Form Factors

In principle one needs two form factors to describe the behaviour of a nucleon – F_1 (the Dirac form factor) describes the deviation of the hadron from a point charge and F_2 (the Pauli form factor) describes the deviation of the hadron from a point anomalous magnetic moment [58]. These are related to the current matrix elements as

$$\langle P'|J^\mu(0)|P\rangle = \bar{u}(P')\left(\gamma^\mu F_1(q^2) + \frac{i\sigma^{\mu\nu}q_\nu}{2\mathcal{M}} F_2(q^2)\right) u(P). \tag{3.150}$$

In the Born approximation of a single exchanged virtual photon between a lepton and a hadron, the scattering amplitude $\mathcal{M}_S$ is related to the leptonic current ℓ_μ and hadronic current $\mathcal{J}_\mu = ie\,\langle P'|J_\mu|P\rangle$ as

$$i\mathcal{M}_S \;=\; \frac{-i}{q^2}\ell_\mu \mathcal{J}^\mu. \tag{3.151}$$

Because one needs to assure the relativistic invariance of $\mathcal{M}_S$, the expression for $\mathcal{J}^\mu$ can only contain the momenta, Dirac matrices, masses and constants, and thus one ends up with the expression (3.150) as the most general expression for $\mathcal{J}^\mu$ satisfying relativistic invariance and current conservation. [73]

In light-front, the form factors can be identified as the spin-conserving and the spin-flip current matrix elements, respectively [39]

$$\langle P',\uparrow|\frac{J^+(0)}{2P^+}|P,\uparrow\rangle \;=\; F_1(q^2), \tag{3.152}$$

$$\langle P',\uparrow|\frac{J^+(0)}{2P^+}|P,\downarrow\rangle \;=\; \frac{iq^2-q^1}{2\mathcal{M}}F_2(q^2). \tag{3.153}$$

These can be also expressed as Sachs form factors G_E and G_M as linear combinations [74, 75]

$$G_E(Q^2) \;=\; F_1(Q^2) - \frac{Q^2}{4\mathcal{M}^2}F_2(Q^2), \tag{3.154}$$

$$G_M(Q^2) \;=\; F_1(Q^2) + F_2(Q^2). \tag{3.155}$$

Sachs form factors clarify the meaning of the form factors: in the non-relativistic limit in the Breit frame (i.e. $P' = -P$), the Fourier transformations of the Sachs form factors are the electric charge density within the nucleus for G_E and the magnetisation density for G_M [75, 76]. In the $Q^2 \to 0$ limit $G_E^p(Q^2 \to 0) = 1$ for proton and $G_E^n(Q^2 \to 0) = 0$ for neutron and $G_M(Q^2 \to 0) = (G_E(0) + F_2(0)) = \mu$, where μ is the magnetic moment. Thus F_2 represents the anomalous magnetic moment. [77]

In the AdS_5 gravity theory, the form factor F_1 of the electromagnetic transition corresponds to a coupling of an external electromagnetic field $A^M(x,z)$ propagating in the bulk with a fermionic mode $\Psi_P(x,z)$, given by the Polchinski-Strassler formula,

$$\int \mathrm{d}^4x\,\mathrm{d}z\sqrt{g}\bar{\Psi}_{P'}e_M^A\Gamma_A A^M\Psi_P \sim (2\pi)^4\delta^{(4)}(P'-P-q)\epsilon_\mu\bar{u}_{P'}\gamma^\mu F_1 u_P. \tag{3.156}$$

When computing nucleon form factors, one should impose boundary conditions so that the leading fall-out of the form factors will match the twist-dimension of the interpolating operator in the asymptotic IR boundary. Here there is a complication: at low energies the strongly correlated, non-perturbative region the bound state of n quarks behaves as a system of one active quark and $n-1$ spectator quarks, thus having twist dimension $\tau = n-1$ (for $L = 0$ state), whereas in the high-energy regime and large momentum transfers, or small distances, the bound state is resolved into its constituents, and thus it has $\tau = n$. At transitional regions, the Dirac form factor for nucleons should therefore evolve from a a quark-diquark $\tau = 2$ to a $\tau = 3$ function. [39]

The resolution between these different twist states is an approximation: the behaviour of form factors is strongly constrained at low energies, and thus we choose to approximate F_1 to have $\tau = 3$ behaviour at all energy ranges, and F_2 to have $\tau = 3 + L = 4$. [39]

To compute the form factors, we incorporate the spin-flavour structure to the light-front holography. It is not necessary – one could build a phenomenological model for a quark-diquark baryon without the flavour structure, as demonstrated in [78].

The incorporation of the spin-flavour structure to the model can be done by using the SU(6) spin-flavour symmetry to weigh the different Fock states by the charges and spin-projections of the quark constituents. In practice, this means weighing the Fock states by probabilities of the constituents to be up or down, $N_{q\uparrow}$ and $N_{q\downarrow}$ respectively. [35, 39]

For proton and neutron these probabilities are [35]

$$p: \qquad N_{u\uparrow} = \frac{5}{3}, \quad N_{u\downarrow} = \frac{1}{3}, \quad N_{d\uparrow} = \frac{1}{3}, \quad N_{d\downarrow} = \frac{2}{3}, \tag{3.157}$$

$$n: \qquad N_{u\uparrow} = \frac{1}{3}, \quad N_{u\downarrow} = \frac{2}{3}, \quad N_{d\uparrow} = \frac{5}{3}, \quad N_{d\downarrow} = \frac{1}{3}, \tag{3.158}$$

where the factors 2 are included in the probabilities.

Following the mesonic example (3.132), the nucleon Dirac form factor can be expressed as

$$F_1^{\pm}(Q^2) = g_{\pm} R^4 \int \frac{\mathrm{d}z}{z^4} V(Q^2, z) \Psi_{\pm}^2, \tag{3.159}$$

where $g_{\pm}$ are effective charges determined by a sum of charges of struck quarks convoluted by the corresponding probability. Thus $g_p^+ = 1$, $g_p^- = 0$, $g_n^+ = -1/3$ and $g_n^- = 1/3$ for $e_u = 2/3$ and $e_d = -1/3$.

For proton and neutron the Dirac form factors are thus

$$\begin{aligned} F_1^p(Q^2) &= F_1^+(Q^2), & (3.160)\\ F_1^n(Q^2) &= \frac{1}{3}\left(F_1^-(Q^2) - F_1^+(Q^2)\right). & (3.161) \end{aligned}$$

The bulk-to-boundary operator is given by (3.138), and the valence LFWFs are given by (3.105) and (3.106) using $\Psi_{\pm} = z^2 \psi_{\pm}$:

$$\Psi_+ = \frac{\sqrt{2}\kappa^2}{R^2} z^{7/2} e^{-\kappa^2 z^2/2}, \quad \Psi_- = \frac{\kappa^3}{R^2} z^{9/2} e^{-\kappa^2 z^2/2}. \tag{3.162}$$

Plugging these in, we find that the expressions for the form factors F_1^+ and F_1^- are exactly the same as for the form factors for $\tau = 3$ and $\tau = 4$ mesons in Equation (3.143), i.e.

$$\begin{aligned} F_1^+(q^2) &= \frac{1}{\left(1 + \frac{Q^2}{\mathcal{M}_\rho}\right)\left(1 + \frac{Q^2}{\mathcal{M}_{\rho'}}\right)}, & (3.163)\\ F_1^-(q^2) &= \frac{1}{\left(1 + \frac{Q^2}{\mathcal{M}_\rho}\right)\left(1 + \frac{Q^2}{\mathcal{M}_{\rho'}}\right)\left(1 + \frac{Q^2}{\mathcal{M}_{\rho''}}\right)}. & (3.164) \end{aligned}$$

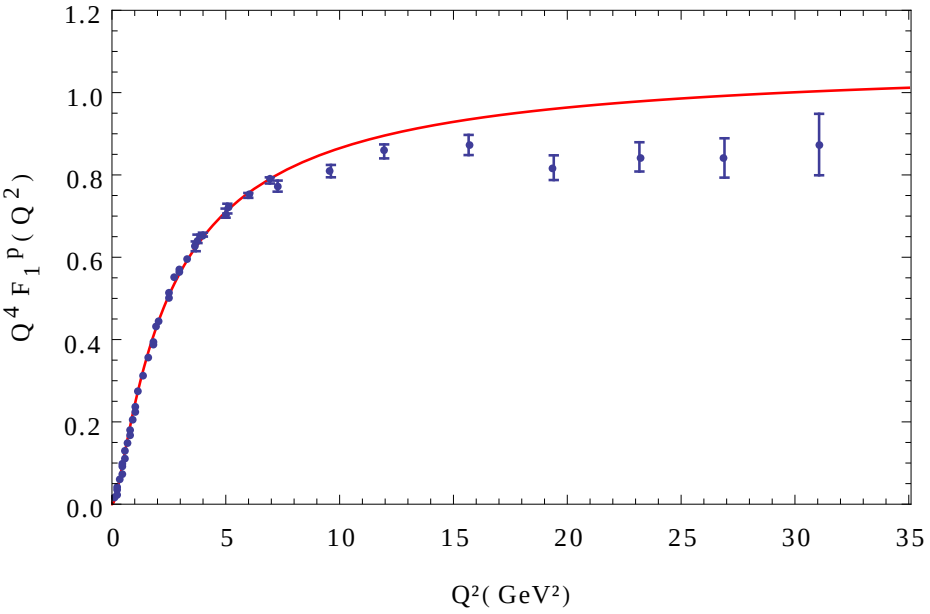

Figure 3.11: The proton elastic Dirac form factor F_1^p times Q^4 as a function of Q^2. Data compilation by [79].

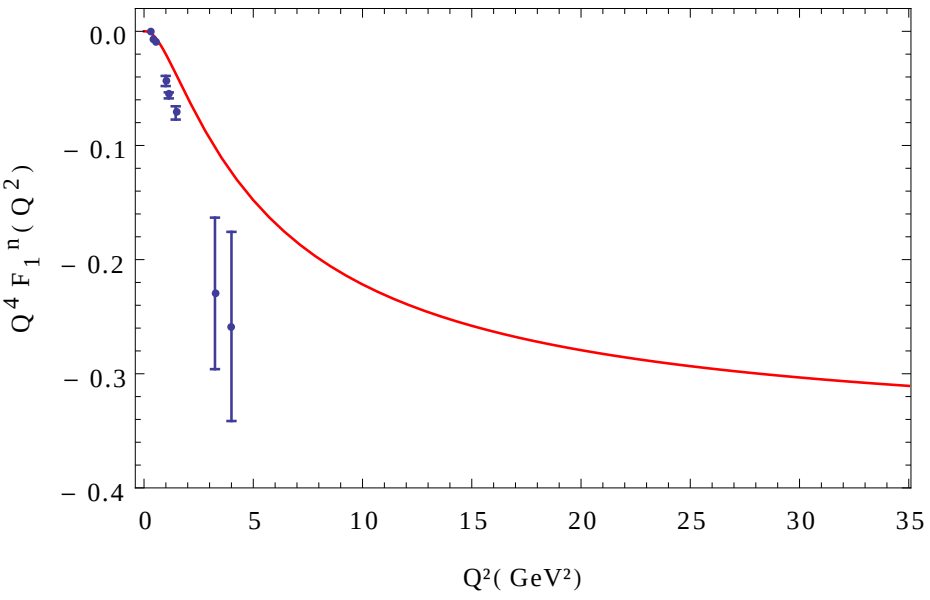

Figure 3.12: The neutron elastic Dirac form factor F_1^n times Q^4 as a function of Q^2. Data compilation by [79].

To study the spin-flip form factor F_2 in the light-front holographic scheme,

Abidin and Carlsson [47] have proposed including a non-minimal coupling

$$\int \mathrm{d}^4x\,\mathrm{d}z\sqrt{g}\bar{\Psi}e^A_M e^B_N\left[\Gamma_A,\Gamma_B\right]F^{MN}\Psi, \tag{3.165}$$

to the 5 dimensional action. The term is rather practical, but it has to be fixed in strength by the static quantities [39].

Using the non-minimal coupling (3.165) and (3.150) one finds

$$\begin{aligned} F_2^{p,n} &\sim \int \frac{\mathrm{d}z}{z^3}\Psi_+ V(Q^2,z)\Psi_- && (3.166)\\ &= \kappa_{p,n}F_1^-(Q^2), && (3.167)\end{aligned}$$

where $\kappa_p = \mu_p - 1$ and $\kappa_n = \mu_n$ are the anomalous magnetic moments. In SU(6), the prediction for the ratio of the magnetic moments is $\mu_p/\mu_n = -3/2$ [80], agreeing with experiments to a high degree of accuracy – the experimental value for the ratio is $\mu_p/\mu_n = -1.45989806(34)$ [81].

Here the experimental values for anomalous magnetics moments

$$\begin{aligned} \kappa_p &= 1.792847356(23), && (3.168)\\ \kappa_n &= -1.91304272(45), && (3.169)\end{aligned}$$

are used [28].

There is some dispute about the scaling behaviour of the G_E^p/G_M^p ratio. The JLab results from double polarization experiments suggest that $R \equiv \mu_p G_E^p/G_M^p$ decreases approximately linearly – approximately $R \approx 1 - 0.135(Q^2 - 0.24)$ [82]– whereas the previous results using the Rosenbluth separation method suggest that for $Q^2 \lesssim 6$ GeV^2, the relation should be $R \approx 1$. The differences between the methods are discussed in detail in Ref. [73]. The discrepancy between the double polarization data and the Rosenbluth method data might be resolved to a degree by two-photon exchange corrections to the Rosenbluth data [83].

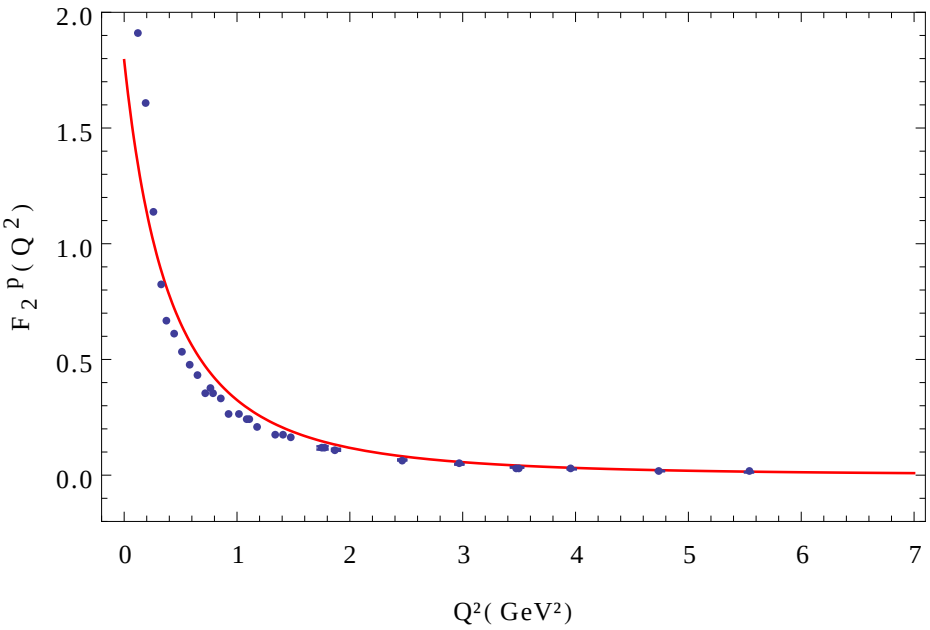

Figure 3.13: The proton elastic Pauli form factor F_2^p as a function of Q^2. Data compilation by [79].

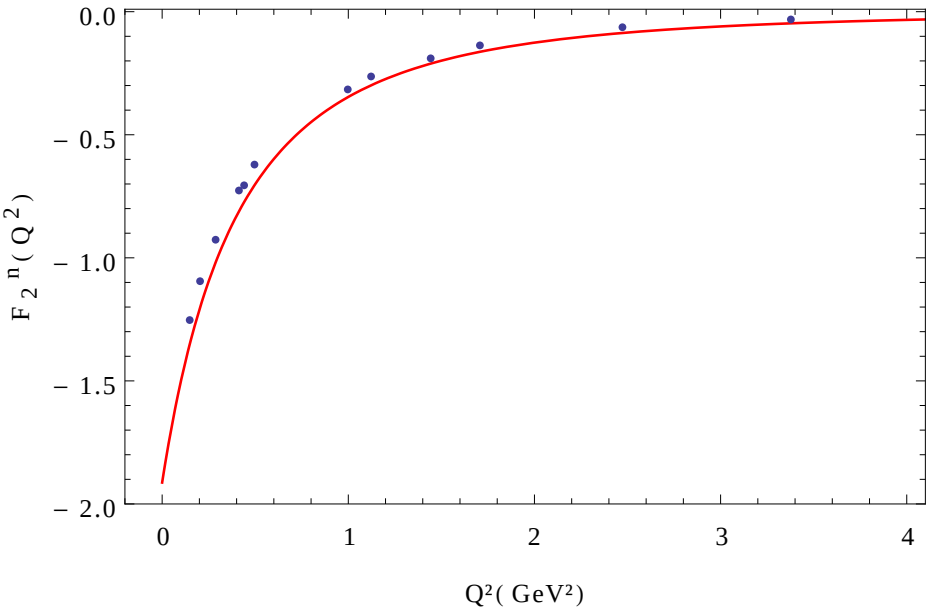

Figure 3.14: The neutron elastic Pauli form factor F_2^n as a function of Q^2. Data compilation by [73].

There is also a dispute about the radii of the proton. The new measurements of the charge radius by the Lamb shift of muonic hydrogen by [84, 85], differ from the electron-proton elastic scattering value by CODATA [81] by 7σ. The most recent values are $\sqrt{\langle r_E^2\rangle}_p = 0.84087(39)$ fm from the muonic hydrogen measurement [85] and $\sqrt{\langle r_E^2\rangle}_p = 0.8775(51)$ fm from e-p scattering [81].

One can compute the electric (or magnetic) charge radius from the electric (or magnetic) Sachs form factor as [35, 78]

$$\langle r^2\rangle = -\frac{6}{G(0)}\left.\frac{\mathrm{d}G(Q^2)}{\mathrm{d}Q^2}\right|_{Q^2=0}. \tag{3.170}$$

This is not simply a definition, as it can be seen by expanding the electric (or magnetic) distribution function at small r [73]. The charge radius for neutron, however is defined as [78]

$$\langle r_E^2\rangle_n = -6\left.\frac{\mathrm{d}G_E^n(Q^2)}{\mathrm{d}Q^2}\right|_{Q^2=0}, \tag{3.171}$$

because $G_E^n(Q^2=0)=0$.

The predictions for the radii in the light-front holography are presented in Table 3.1. [1]

	Prediction	$CODATA$ value	μp value
$(\langle r_E^2\rangle_p)^{1/2}$	0.7783	0.8775 ± 0.0051	0.84087 ± 0.00039
$(\langle r_M^2\rangle_p)^{1/2}$	0.754	0.777 ± 0.016	0.87 ± 0.06
$\langle r_E^2\rangle_n$	-0.0671	-0.1161 ± 0.0022	
$(\langle r_M^2\rangle_n)^{1/2}$	0.763	$0.862^{+0.009}_{-0.008}$	

Table 3.1: The charge and magnetic root mean square radii for nucleons in light-front compared to the experimental values. The experimental values are from References [28] and [85] respectively. All values are in femtometres except for $\langle r_E^2\rangle_n$, which is in fm^2. The value of κ is chosen to be the same as all the other soft-wall holographic form factor calculations, $\kappa = 0.548$.

[1] We know the disagreement between the results presented here and the ones presented in e.g. references [35, 39]. It does not seem to arise purely from the choice of κ, as the values do not match even for identical κ.

The values for proton agree better with experimental results than the ones for neutron. This is in line with the proton Dirac form factor fitting better with the experimental results (Figure 3.11) compared to the fit of the neutron Dirac form factor (Figure 3.12).

3.6 Improving the Model

The full description of the light-front holographic approach is far from being understood. This is clearly visible from the approximations and *ad hoc* elements introduced to the theory along the way in this chapter. The semiclassical approximation is expected to break down when gluons become dynamical degrees of freedom and when quantum corrections become important.

To go further, one would need to improve the semi-classical approximation by e.g. including higher Fock states $|n\rangle$ (i.e. quantum fluctuations), including quark masses and introducing gluon exchange to the model.

Including the quark masses m_q and $m_{\bar{q}}$ to the mass of a $n = 2$ meson in the soft-wall model can be done by introducing a shift term $\Delta\mathcal{M}^2$ such that

$$\mathcal{M}^2_{n,J,L,m_q,m_{\bar{q}}} = 4\kappa^2 \left(n + \frac{J+L}{2}\right) + \Delta\mathcal{M}^2, \tag{3.172}$$

with the correction being [39]

$$\Delta\mathcal{M}^2 = \langle\psi| \sum_a m_a^2/x_a |\psi\rangle \,. \tag{3.173}$$

For baryons, incorporating quark masses to the model is not as straightforward, as for massive fields left- and right-handed fermions are not independent. [47]

Other required improvements still have no solutions. The problems with the model include finding a way to include isoscalar mesons to the model, fixing the a meson triplet splitting masses, finding a non-phenomenological way to include the Pauli form factor into the theory so that one does not need to use the anomalous magnetic moments as experimental inputs but would get them from the model itself. Also, the assignment of ν for baryons is purely phenomenological, as the dilaton does not lead to a confining potential but it has to be imposed upon. And the nucleons are not accounted for as

twist-3 states in the short-distance regime as they should because of cluster decomposition resolving.

Chapter 4

A Model of Composite Dark Matter

In this Chapter, an application of the light-front holographic QCD is realised in a model of composite dark matter, where a new strongly interacting secluded sector is introduced. The first section offers a brief review on the subject of dark matter: observations backing up its existence, which models are favoured and direct detection experiments. The later Sections develop on the idea of composite dark matter, look into its properties and compare it with direct detection experiments.

4.1 A Word About Dark Matter

One of the most astounding results of the 20th century cosmology has been the realisation that visible matter only accounts for about 5% of the total energy density of the observable universe. 68% is made of elusive *dark energy* and about 27% of non-luminous *dark matter*. [86] By now, dark matter (DM) enjoys the consensus of the scientific community, even as we have no confirmed direct detection of it – only the DAMA/LIBRA [87] and CoGeNT [88] experiments claim to see an annual modulation signal, which other experiments have excluded [89].

4.1.1 Observational Evidence for Existence

The first correct observational evidence that either the gravitational theory at large distances could be wrong or that we cannot see a major mass component of the universe came from Fritz Zwicky in 1933 [90]: the velocities of galaxies in the Coma cluster were much greater than the escape velocity from the cluster based on the visible mass of the cluster. Also, the rotation curve does not obey the radial Keplerian fall $v \propto 1/r$, but turns approximately flat at large r. Later observations have confirmed the observation (e.g. [91]) and seen similar behaviour with different galaxy clusters like Virgo. [92]

One of the most convincing single observation for DM comes from merging galaxy clusters like 1E0657-558 [93] , also known as the Bullet Cluster, and MACS J0025.4-1222 [94]. In the collision of two galaxy clusters the stellar component – which is non-dissipative – and the interstellar gas – which is fluid-like and emits X-rays – are segregated. The observations have shown the gravitational potential traces approximately the distribution of galaxies, not the gas component which is the dominant baryonic mass component [93].

Other indirect evidence for the existence of dark matter include the gravitational lensing effect around galaxy clusters, which cannot be accounted for by visible mass only.

4.1.2 The Dark Matter Problem

Some of the DM might be accounted for by baryonic matter like interstellar gas or massive astrophysical compact halo objects (MACHOs), which includes compact objects like black holes, brown dwarfs, old white dwarfs and neutron stars. The main evidence against baryonic matter making up a considerable amount of DM is found in the cosmic microwave background (CMB): anisotropies of CMB suggest that most of the matter content of the Universe does not interact substantially with ordinary matter [95].The microlensing searches are also against MACHOs making a non-negligible amount of DM [96].

The non-baryonic candidates can be divided into three groups: cold dark matter (CDM), warm dark matter (WDM) and hot dark matter (HDM). CDM is non-relativistic at decoupling, and thus is suppressed in number

density by annihilation and needs to be heavy to compensate for the small number density. HDM on the other hand should be fairly light, as it is relativistic at decoupling. WDM is between these two ends. Of these, the CDM scenario produces a model best consistent with the observed universe for example from the standpoint of structure formation [97].

One might of course argue that the DM problem is a sign of the incompetence of General Relativity as all the observational evidence is gravity based, and that the theory of gravity should be modified at cosmological scales. This is of course a point of view worth considering, but the ΛCDM model is predictive, whereas gravity needs to be adjusted differently in the different systems. And thereby DM is a favourite contender to solve the discrepancy. Moreover, the corrections needed to explain the lensing effect around previously mentioned merging clusters requires modifying the gravity so that most of the lensing is not where most of the mass is. However, to truly make a case for the existence of DM over other models like modified gravity, there should be a body of direct detection evidence for its existence via non-gravitational interactions.

Even though the ΛCDM paradigm is predictive at cosmological scales, it has its pitfalls, like the "cusp vs core" problem with dwarf galaxies [98, 99]. Some of the problems might be fixed by improving the ΛCDM simulations by, for example, including baryonic effects [100].

4.1.3 Exclusions from Direct Detection Experiments

Direct detection of DM is based on trying to observe scattering between a non-relativistic DM particle from the halo of our galaxy and a cryogenic nucleus or the orbital electrons of the detector. To distinguish the signal from the background, one needs to look for an annual modulation in the detection rate as the Earth is moving with respect to the velocity distribution of the DM.

We will focus on the elastic scattering, i.e. the scattering between the DM particle and the nucleus. The scattering can then be either spin-dependent or spin-independent. In the spin-dependent scattering the interaction between the two particles is caused by the coupling of the DM particle to the nucleon's

spin, whereas in the spin-independent the two are not coupled.

Multiple experiments, including XENON, CDMS, ZEPLIN, EDELWEISS, COUPP, CRESST, DAMA, CoGeNT, SIMPLE, WARP, ORPHEUS, KAMIOKA, NEWAGE, PICASSO, IGEX, HDMS, NAIAD and KIMS, are (or have been) trying to detect the elastic scattering signal, and have by now put stringent constraints on WIMP-nucleon scattering. [89, 92] Most of their results are gathered in Figure 4.1, with assumptions of the isothermal distribution of DM in the halo being $v_0 = 220$ km/s, the galactic escape velocity being $v_{esc} = 544^{+64}_{-46}$ km/s and the WIMP density being $\rho_{DM} = 0.3$ GeV/cm^3 [89].

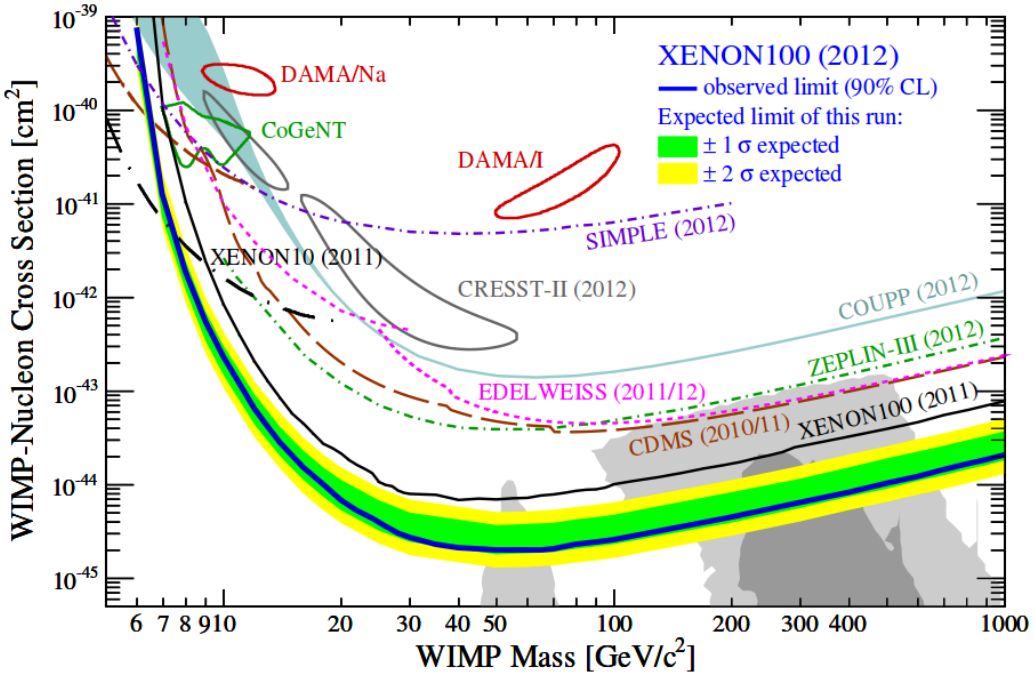

Figure 4.1: Exclusions on spin-independent WIMP-nucleon scattering from XENON100. Source [89]

4.2 Proposing a New Strongly Interacting Sector

As we have no undisputed direct detection of dark matter and thus we do not know what exactly it is comprised of, Occam's razor does not carry us

far – minimality might not be the best guide when trying to find a model for dark matter. We do know that dark matter is not from the Standard Model of particle physics, but when modelling something left in the dark, we can use our existing models as a basis to build upon.

It is more than reasonable to build the *secluded sector* out of the building blocks the Standard Model of particle physics (SM) also comprises of. We can make the secluded sector so that it has some of the same symmetries as the SM, but they interact with each other only weakly. To make the use of terminology clear, when in this thesis the term "weakly" is used, it does not mean "via Weak interaction" but that the interactions – whatever they are – are weak. So, WIMPs interact weakly with the Standard Model particles through electromagnetism.

The procedure is to modify the SM by introducing a new SU(3) symmetry to the theory (a secluded sector), the fundamental particles of which are thus analogues of quarks and gluons. There are multiple ways to formulate the interactions of the secluded sector with the standard model. Here we assume the secluded sector particles couple to the SM electromagnetic field like their SM analogues and also communicate with the SM via the Higgs portal. Thus, the dark quarks are $\mathrm{SU}(2)_L$ singlet states with $Q = Y$ with other values matching those of the SM quarks.

The lightest baryonic state is the dark neutron and it is our dark matter candidate, which will be noted with χ. It is stable, unlike its SM counterpart, because the dark baryon number is conserved. The lightness of the neutron is a result of the assumption of unbroken isospin symmetry: the dark neutron and the dark proton have the same mass without electromagnetic corrections. The electromagnetic corrections raise the mass of the dark proton to $M_{dp} = (1 + \alpha_{\mathrm{EM}}/4\pi)M_\chi \approx M_\chi$. This gives us a lower limit for the mass of the dark neutron, as one would expect to see a reasonably light charged particle, with mass $\mathcal{O}(\mathrm{TeV})$ in the collider experiments. However, we will later see that the region, where the collider constraints are significant, is already secluded by direct detection searches.

Regarding the origin of the DM candidate in question, there are two possibilities: either the relic abundance is determined thermally as in the usual “WIMP miracle” or by a primordial asymmetry through the same early

universe sphaleron process describing baryogenesis [101–103]. To consider the origin of the DM, and the relation of the model to the electroweak symmetry breaking, the model would need to be set into a larger context.

Here the cosmological history will be left unspecified and the distribution and abundance of DM in our galaxy is taken as given, so the focus can be set on the direct detection signature of the composite dark matter in question. The direct detection of DM is based on observing the elastic scattering between a cryogenic target nuclei and the non-relativistic DM in our galaxy's halo. Because the dark neutron state is electroweak-neutral as a totality, the main contribution to direct detection of such a particle would be via single photon exchange, the Feynman diagram of which is in Figure 4.2b. The spin-independent interaction is simply an exchange of a Higgs boson, which conserves the spin of both particles. The spin-dependent interaction happens via a single-photon exchange in the simplest scenario.

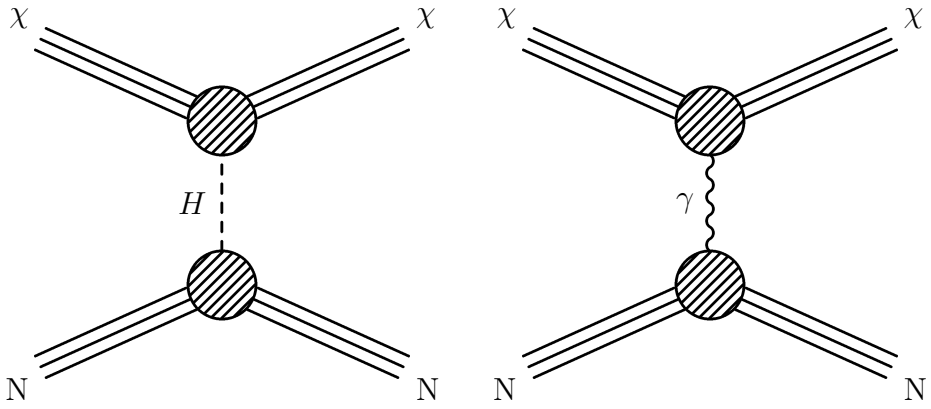

(a) Spin-independent interaction of a composite dark matter particle and a nucleon via a Higgs exchange.

(b) Spin-dependent interaction of a composite dark matter particle and a nucleon via a single photon exchange.

Figure 4.2: The Feynman diagrams for the composite dark matter χ interacting with a nucleon N via the Higgs channel **(a)** and the EM channel **(b)**. The Higgs exchange does not affect the spins of the particles, whereas the photon exchange does flip the spins.

The LSD Collaboration has done similar lattice simulations [103], and we will compare our results to theirs in the end of the chapter. Other models considering strongly interacting dark matter in the form of Technicolor DM

or atomic DM can be found e.g. in references [102, 104–113].

Assuming non-relativistic DM, the differential cross-section of the elastic scattering can be written as [103]

$$\frac{\mathrm{d}\sigma}{\mathrm{d}E_R} = \frac{\overline{|\mathcal{M}_{SI}|^2} + \overline{|\mathcal{M}_{SD}|^2}}{16\pi \left(M_\chi + M_T\right)^2 E_R^{\max}}, \tag{4.1}$$

where $\mathcal{M}_{SI/SD}$ are the spin-independent and spin-dependent amplitudes, M_T is the mass of the target nucleus and $E_R^{\max} = 2M_\chi^2 M_T v^2/(M_\chi + M_T)^2$ is the maximum recoil energy for a collision velocity v. The amplitudes squared, averaged over the initial states and summed over the final states are given by [103]

$$\begin{aligned}
\overline{|\mathcal{M}_{SI}|^2} &= e^4 \left[Z F_c(Q)\right]^2 \left(\frac{M_T}{M_\chi}\right)^2 \left[\frac{4}{9} M_\chi^4 \left\langle r_{E\chi}^2 \right\rangle^2 \right. \\
&\quad \left. + \left(1 + \frac{M_\chi}{M_T}\right)^2 \kappa_\chi^2 \cot^2 \frac{\theta_{\mathrm{CM}}}{2}\right], \qquad (4.2) \\
\overline{|\mathcal{M}_{SD}|^2} &= e^4 \frac{2}{3} \left(\frac{J+1}{J}\right) \left[A \mu_T F_s(Q)\right]^2 \kappa_\chi^2, \qquad (4.3)
\end{aligned}$$

where κ_χ is the magnetic moment of χ, A and Z are the atomic and mass numbers of a specific xenon isotope, θ_{CM} is the scattering angle in the center-of-mass frame, J is the nuclear spin of the target, and $F_{s,c}$ are the nuclear spin form factor and form factor accounting for the loss of coherence, respectively. The magnetic moment μ_T of the target is expressed in units of Bohr magnetons. For non-relativistic velocities $\cot^2 \frac{\theta_{\mathrm{CM}}}{2} = E_R^{\max}/E_R - 1$. The momentum exchange can be estimated to be $Q \approx \sqrt{2 M_T E_R}$.

We know the mean squared charge radius $\langle r_{E\chi}^2 \rangle$ for χ from (3.171) and the mass M_χ from (3.108) for a given κ.

For the nuclear response form factors $F_{c,s}$, we use the phenomenological expressions [114]

$$\begin{aligned}
|F_c(Q)|^2 &= 9 \left[\frac{\sin(QR_c) - QR_c \cos(QR_c)}{(QR_c)^3}\right]^2 \mathrm{e}^{-iQ^2 s^2}, \qquad (4.4) \\
|F_s(Q)|^2 &= \begin{cases} 0.047 & \text{for } 2.55 \le QR_s \le 4.5, \\ (QR_s)^{-2} \sin^2(QR_s) & \text{otherwise}, \end{cases} \qquad (4.5)
\end{aligned}$$

with $R_c = 1.14 A^{1/3}$ fm, $R_s = A^{1/3}$ fm and $s = 0.9$ fm.

We take the velocity-averaged differential cross section of the DM interaction weighted by the DM velocity, $v' = |\mathbf{v} - \mathbf{v}_E|$ with respect to Earth to be

$$\left\langle \frac{\mathrm{d}\sigma}{\mathrm{d}E_R} v' \right\rangle = \int_0^{v_{\max}} \mathrm{d}v' f(\mathbf{v}) v' \frac{\mathrm{d}\sigma}{\mathrm{d}E_R}, \tag{4.6}$$

where the velocity distribution is assumed to be the Maxwell-Boltzmann distribution in the galactic rest frame [115]

$$f_{\text{galaxy}}(\mathbf{v}) = \frac{\exp(-\mathbf{v}^2/v_0^2)}{\pi^{3/2} v_0^3}, \tag{4.7}$$

with the most probable velocity being $v_0 = 220$ km/s and the escape velocity $v_{\text{esc}} = 544$ km/s. The velocity distribution in Earth's frame is obtained via a Galilean transformation, [114, 116]

$$f(\mathbf{v}) = \begin{cases} \dfrac{v}{\sqrt{\pi} v_0 v_E} \left[\mathrm{e}^{-v'^2/v_0^2} - \mathrm{e}^{-(v+v_E)^2/v_0^2} \right] & \text{for } 0 \leq v \leq v_{\text{esc}} - v_E, \\ \dfrac{v}{\sqrt{\pi} v_0 v_E} \left[\mathrm{e}^{-v'^2/v_0^2} - \mathrm{e}^{-v_{\text{esc}}^2/v_0^2} \right] & \text{for } v_{\text{esc}} - v_E < v \leq v_{\text{esc}} + v_E, \end{cases} \tag{4.8}$$

with the speed of Earth approximated by $v_E = 220$ km/s. If one would like to see the annular modulation in the event rate instead of acquiring limits to a model, the velocity should have a periodic term in it (see e.g. references [114, 115]).

The quantity measured in experiments is the event rate, and this can be acquired from the averaged differential cross section times velocity as [103]

$$R = \frac{M_{\text{detector}}}{M_T} \frac{\rho_{DM}}{M_\chi} \int_{E_{\min}}^{E_{\max}} \mathrm{d}E_R \mathcal{A}(E_R) \left\langle v' \frac{\mathrm{d}\sigma}{\mathrm{d}E_R} \right\rangle, \tag{4.9}$$

where $\mathcal{A}$ and is the acceptance function of the detector.

4.3 Results

Let us now try to fit the model using the XENON100 experiment. For xenon $Z = 54$ and $A = 124 - 136$. Only two of the isotopes of xenon have non-zero spins: ^{129}Xe ($J = 1/2$) and ^{131}Xe ($J = 3/2$), thus being the only isotopes contributing to the spin-dependent scattering [117]. The event rate

is computed in the recoil energy interval $E_R \in [6.6\text{keV}, 43.3\text{keV}]$ following references [89, 103, 114]. The masses of different isotopes are approximated to be $M_T \approx A$ atomic mass units and all rates are averaged over the different isotopes by weighing them with their respective abundances taken from [118].

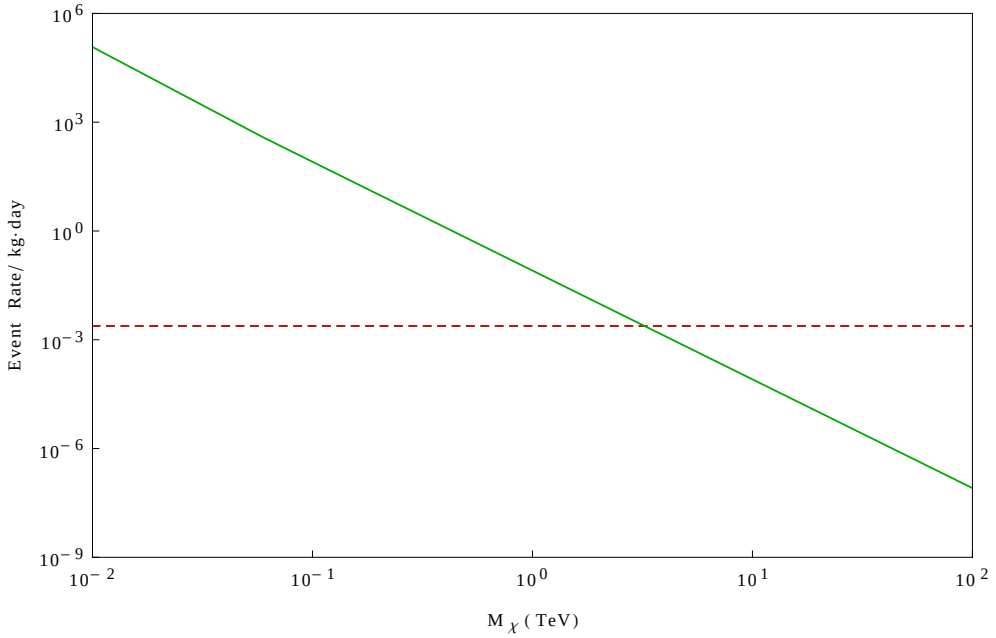

Figure 4.3: The predicted event rate for a kilogram of liquid xenon per day as a function of the mass of the composite dark matter particle. The dashed red line marks the 95% exclusion from the XENON100 experiment [89]. The possible masses of the composite DM particle are thus above the $M_\chi \sim 5$ TeV limit.

The results were computed numerically from $M_\chi = 10^{-2}$ TeV to $M_\chi = 10^2$ TeV in increments of 50 GeV (Figure 4.3). The model produces a linear regression in the log-log plot and agrees well with the lattice simulations of the LSD collaboration [103] for the large mass region, but does not exhibit similar behaviour at masses around 10^{-2} TeV. The XENON100 experiment excludes masses below $M_\chi \sim 5$ TeV for this model.

Chapter 5

Conclusions And Discussion

In this thesis, the light-front holographic QCD was studied and its properties discussed in the light of contemporary literature. It encodes to a good accuracy some of the most important aspects of non-perturbative QCD, like confinement and the hadron mass spectrum. Some discrepancies with previous works were found, as the charge and magnetic radii computed for this work are in conflict with existing literature. However, the light-front holographic QCD does provide a first approximation that agrees with the experimental data where the model is applicable. More importantly, it can be improved upon by, for example, including light quark masses, more Fock-states and gluon exchange.

The successful application of holographic methods to QCD also speaks for using the AdS/CFT correspondence to study strongly coupled systems. Of course, the approach used in this work was more or less *ad hoc* in building the gravity dual, but one can always hope that a more rigorous way of applying the duality can be found in the future.

An application of the light-front holographic model was found in composite dark matter. The studied model comprises of a secluded SU(3) gauge theory with $SU(2)_L$-singlet fermions analogous to QCD, that make up a stable, electroweak neutral baryon that is the WIMP candidate. It exhibits the desired properties, as it will interact weakly via the electroweak channel and will need to have a mass of over 5 TeV to satisfy the XENON100 exclusions. The results from the model agree with previous work by [103] for appropriate

mass scales.

One of the more serious problems regarding the applicability of light-front holographic QCD to the model of composite dark matter discussed in this thesis is the fact that one needs to take the neutron anomalous magnetic moment as an input. The value of the magnetic moment has a substantial effect on the results, and therefore acquiring it from the theory would be of critical importance, especially if one wants to assign microcharges to the secluded sector quarks instead of using the SM charges.

In this work the dark matter genesis was not speculated on, and it was assumed that the cosmological history stays roughly as it is in the vanilla ΛCDM model, although via the secluded SU(3) sector there is a possibility to link the dark matter genesis to baryogenesis [102]. The model has three pseudo-Nambu-Goldstone bosons (dark pions), and one needs to assume that they are highly unstable and decay into SM particles without a notable impact on the cosmological history. Calculating the effects of dark pions is a subject for possible future work.

Bibliography

[1] S. J. Brodsky, H.-C. Pauli, and S. S. Pinsky: "Quantum chromodynamics and other field theories on the light cone". *Phys.Rept.* **301**, 299–486 (1998). arXiv:hep-ph/9705477

[2] P. A. Dirac: "Forms of Relativistic Dynamics". *Rev.Mod.Phys.* **21**, 392–399 (1949)

[3] J. M. Maldacena: "The Large N limit of superconformal field theories and supergravity". *Adv.Theor.Math.Phys.* **2**, 231–252 (1998). arXiv:hep-th/9711200

[4] R. Bousso: "The Holographic principle". *Rev.Mod.Phys.* **74**, 825–874 (2002). arXiv:hep-th/0203101

[5] O. Aharony et al.: "Large N field theories, string theory and gravity". *Phys.Rept.* **323**, 183–386 (2000). arXiv:hep-th/9905111

[6] G. 't Hooft: "Dimensional reduction in quantum gravity" (1993). arXiv:gr-qc/9310026

[7] C. B. Thorn: "Reformulating string theory with the 1/N expansion" (1991). arXiv:hep-th/9405069

[8] L. Susskind: "Strings, black holes and Lorentz contraction". *Phys.Rev.* **D49**, 6606–6611 (1994). arXiv:hep-th/9308139

[9] S. Hawking: "Gravitational radiation from colliding black holes". *Phys.Rev.Lett.* **26**, 1344–1346 (1971)

[10] J. D. Bekenstein: "Black holes and entropy". *Phys.Rev.* **D7**, 2333–2346 (1973)

[11] I. R. Klebanov and L. Susskind: "Continuum Strings From Discrete Field Theories". *Nucl.Phys.* **B309**, 175 (1988)

[12] H. G. Dosch: *A Practical Guide to AdS/CFT*. `http://www.thphys.uni-heidelberg.de/~dosch/wuhantot.pdf`. [Lectures given at the School of Physics and Technology, Wuhan University]. 2009

[13] E. Witten: "Bound states of strings and p-branes". *Nucl.Phys.* **B460**, 335–350 (1996). arXiv:`hep-th/9510135`

[14] M. Schottenloher: *A Mathematical Introduction into Conformal Field Theory*. 2nd ed. Lecture Notes of Physics **759**. Springer-Verlag, 2008

[15] V. de Alfaro, S. Fubini, and G. Furlan: "Conformal Invariance in Quantum Mechanics". *Nuovo Cim.* **A34**, 569 (1976)

[16] E. Witten: "Anti-de Sitter space and holography". *Adv.Theor.Math.Phys.* **2**, 253–291 (1998). arXiv:`hep-th/9802150`

[17] S. Gubser, I. R. Klebanov, and A. M. Polyakov: "Gauge theory correlators from noncritical string theory". *Phys.Lett.* **B428**, 105–114 (1998). arXiv:`hep-th/9802109`

[18] J. M. Maldacena: "TASI 2003 lectures on AdS / CFT", 155–203 (2003). arXiv:`hep-th/0309246 [hep-th]`

[19] H. D. Politzer: "Reliable Perturbative Results for Strong Interactions?" *Phys.Rev.Lett.* **30**, 1346–1349 (1973)

[20] D. J. Gross and F. Wilczek: "Ultraviolet Behavior of Nonabelian Gauge Theories". *Phys.Rev.Lett.* **30**, 1343–1346 (1973)

[21] H. D. Politzer: "Asymptotic Freedom: An Approach to Strong Interactions". *Phys.Rept.* **14**, 129–180 (1974)

[22] D. J. Gross: "Twenty five years of asymptotic freedom". *Nucl.Phys.Proc.Suppl.* **74**, 426–446 (1999). arXiv:`hep-th/9809060`

[23] S. Bethke: "The 2009 World Average of $\alpha(s)$". *Eur.Phys.J.* **C64**, 689–703 (2009). arXiv:`0908.1135 [hep-ph]`

[24] A. S. Kronfeld and C. Quigg: "Resource Letter: Quantum Chromodynamics". *Am.J.Phys.* **78**, 1081–1116 (2010). arXiv:`1002.5032 [hep-ph]`

[25] S. Kluth: "Tests of Quantum Chromo Dynamics at e+ e- Colliders". *Rept.Prog.Phys.* **69**, 1771–1846 (2006). arXiv:hep-ex/0603011

[26] V. Abazov et al. (D0 Collaboration): "Measurement of the inclusive jet cross-section in $p\bar{p}$ collisions at $s^{(1/2)}$ =1.96-TeV". *Phys.Rev.Lett.* **101**, 062001 (2008). arXiv:0802.2400 [hep-ex]

[27] G. Aad et al. (ATLAS Collaboration): "Measurement of the inclusive jet cross section in pp collisions at sqrt(s)=2.76 TeV and comparison to the inclusive jet cross section at sqrt(s)=7 TeV using the ATLAS detector". *Eur.Phys.J.* **C73**.8, 2509 (2013). arXiv:1304.4739 [hep-ex]

[28] K. Olive et al. (Particle Data Group): "Review of Particle Physics". *Chin.Phys.* **C38**, 090001 (2014)

[29] J. M. Campbell, J. Huston, and W. Stirling: "Hard Interactions of Quarks and Gluons: A Primer for LHC Physics". *Rept.Prog.Phys.* **70**, 89 (2007). arXiv:hep-ph/0611148

[30] T. Heinzl: "Light cone quantization: Foundations and applications". *Lect.Notes Phys.* **572**, 55–142 (2001). arXiv:hep-th/0008096

[31] A. Harindranath: "An Introduction to light front dynamics for pedestrians" (1996). arXiv:hep-ph/9612244

[32] S. J. Brodsky and G. F. de Téramond: "The AdS/CFT Correspondence and Light-Front QCD". *PoS* **LC2008**, 044 (2008). arXiv:0810.1876 [hep-ph]

[33] P. P. Srivastava and S. J. Brodsky: "A Unitary and renormalizable theory of the standard model in ghost free light cone gauge". *Phys.Rev.* **D66**, 045019 (2002). arXiv:hep-ph/0202141

[34] S. J. Brodsky, G. F. de Téramond, and H. G. Dosch: "QCD on the Light-Front – A Systematic Approach to Hadron Physics". *Few Body Syst.* **55**, 407–423 (2014). arXiv:1310.8648 [hep-ph]

[35] G. F. de Téramond and S. J. Brodsky: "Hadronic Form Factor Models and Spectroscopy Within the Gauge/Gravity Correspondence" (2012). arXiv:1203.4025 [hep-ph]

[36] J. Erlich et al.: "QCD and a holographic model of hadrons". *Phys.Rev.Lett.* **95**, 261602 (2005). arXiv:hep-ph/0501128

[37] L. Da Rold and A. Pomarol: "Chiral symmetry breaking from five dimensional spaces". *Nucl.Phys.* **B721**, 79–97 (2005). arXiv:hep-ph/0501218

[38] G. F. de Téramond and S. J. Brodsky: "Hadronic spectrum of a holographic dual of QCD". *Phys.Rev.Lett.* **94**, 201601 (2005). arXiv:hep-th/0501022

[39] S. J. Brodsky et al.: "Light-Front Holographic QCD and Emerging Confinement" (2014). arXiv:1407.8131 [hep-ph]

[40] S. J. Brodsky and G. F. de Téramond: "Hadronic spectra and light-front wavefunctions in holographic QCD". *Phys.Rev.Lett.* **96**, 201601 (2006). arXiv:hep-ph/0602252

[41] S. J. Brodsky and G. F. de Téramond: "Light-Front Dynamics and AdS/QCD Correspondence: Gravitational Form Factors of Composite Hadrons". *Phys.Rev.* **D78**, 025032 (2008). arXiv:0804.0452 [hep-ph]

[42] G. F. de Téramond, H. G. Dosch, and S. J. Brodsky: "Kinematical and Dynamical Aspects of Higher-Spin Bound-State Equations in Holographic QCD". *Phys.Rev.* **D87**.7, 075005 (2013). arXiv:1301.1651 [hep-ph]

[43] J. Polchinski and M. J. Strassler: "Deep inelastic scattering and gauge / string duality". *JHEP* **0305**, 012 (2003). arXiv:hep-th/0209211

[44] S. Drell and T.-M. Yan: "Connection of Elastic Electromagnetic Nucleon Form-Factors at Large Q^2 and Deep Inelastic Structure Functions Near Threshold". *Phys.Rev.Lett.* **24**, 181–185 (1970)

[45] G. B. West: "Phenomenological model for the electromagnetic structure of the proton". *Phys.Rev.Lett.* **24**, 1206–1209 (1970)

[46] Z. Abidin and C. E. Carlson: "Gravitational form factors of vector mesons in an AdS/QCD model". *Phys.Rev.* **D77**, 095007 (2008). arXiv:0801.3839 [hep-ph]

[47] Z. Abidin and C. E. Carlson: "Nucleon electromagnetic and gravitational form factors from holography". *Phys.Rev.* **D79**, 115003 (2009). arXiv:0903.4818 [hep-ph]

[48] T. Gutsche et al.: "Dilaton in a soft-wall holographic approach to mesons and baryons". *Phys.Rev.* **D85**, 076003 (2012). arXiv:1108.0346 [hep-ph]

[49] L. Infeld: "On a New Treatment of Some Eigenvalue Problems". *Phys. Rev.* **59**, 737–747 (1941). URL: http://link.aps.org/doi/10.1103/PhysRev.59.737

[50] S. J. Brodsky and G. F. de Téramond: "AdS/CFT and Light-Front QCD" (2008). arXiv:0802.0514 [hep-ph]

[51] S. J. Brodsky and G. F. de Téramond: "Applications of AdS/QCD and Light-Front Holography to Baryon Physics". *AIP Conf.Proc.* **1388**, 22–33 (2011). arXiv:1103.1186 [hep-ph]

[52] A. Karch et al.: "On the sign of the dilaton in the soft wall models". *JHEP* **04**, 066 (2011). arXiv:1012.4813 [hep-ph]

[53] S. J. Brodsky and G. F. de Téramond: "Light-Front Dynamics and AdS/QCD Correspondence: The Pion Form Factor in the Space- and Time-Like Regions". *Phys.Rev.* **D77**, 056007 (2008). arXiv:0707.3859 [hep-ph]

[54] S. J. Brodsky et al.: "The Light-Front Schrödinger Equation and Determination of the Perturbative QCD Scale from Color Confinement" (2014). arXiv:1410.0425 [hep-ph]

[55] H. Hata et al.: "Baryons from instantons in holographic QCD". *Prog.Theor.Phys.* **117**, 1157 (2007). arXiv:hep-th/0701280

[56] D. K. Hong et al.: "Chiral Dynamics of Baryons from String Theory". *Phys.Rev.* **D76**, 061901 (2007). arXiv:hep-th/0701276

[57] R. Feynman: *Photon-hadron interactions*. Benjamin, Reading (Mass.), 1972. ISBN: ISBN-9780201360745

[58] C. Perdrisat, V. Punjabi, and M. Vanderhaeghen: "Nucleon Electromagnetic Form Factors". *Prog.Part.Nucl.Phys.* **59**, 694–764 (2007). arXiv:hep-ph/0612014

[59] D. D. Dietrich, P. Hoyer, and M. Järvinen: "Boosting equal time bound states". *Phys.Rev.* **D85**, 105016 (2012). arXiv:1202.0826 [hep-ph]

[60] D. E. Soper: "The Parton Model and the Bethe-Salpeter Wave Function". *Phys.Rev.* **D15**, 1141 (1977)

[61] S. Hong, S. Yoon, and M. J. Strassler: "On the couplings of vector mesons in AdS / QCD". *JHEP* **0604**, 003 (2006). arXiv:hep-th/0409118

[62] G. Arfken and H. Weber: *Mathematical methods for physicists, 6th ed.* Elsevier Acad. Press, 2005. ISBN: 0-12-088584-0

[63] P. Masjuan, E. Ruiz Arriola, and W. Broniowski: "Meson dominance of hadron form factors and large-N_c phenomenology". *Phys.Rev.* **D87**.1, 014005 (2013). arXiv:1210.0760 [hep-ph]

[64] M. Fujikawa et al. (Belle Collaboration): "High-Statistics Study of the $\tau^- \to \pi^-\pi^0\nu(\tau)$ Decay". *Phys.Rev.* **D78**, 072006 (2008). arXiv:0805.3773 [hep-ex]

[65] F. Ambrosino et al. (KLOE Collaboration): "Measurement of $\sigma(e^+e^- \to \pi^+\pi^-\gamma(\gamma))$ and the dipion contribution to the muon anomaly with the KLOE detector". *Phys.Lett.* **B670**, 285–291 (2009). arXiv:0809.3950 [hep-ex]

[66] F. Ambrosino et al. (KLOE Collaboration): "Measurement of $\sigma(e^+e^- \to \pi^+\pi^-)$ from threshold to 0.85 GeV^2 using Initial State Radiation with the KLOE detector". *Phys.Lett.* **B700**, 102–110 (2011). arXiv:1006.5313 [hep-ex]

[67] D. Babusci et al. (KLOE Collaboration): "Precision measurement of $\sigma(e^+e^- \to \pi^+\pi^-\gamma)/\sigma(e^+e^- \to \mu^+\mu^-\gamma)$ and determination of the $\pi^+\pi^-$ contribution to the muon anomaly with the KLOE detector". *Phys.Lett.* **B720**, 336–343 (2013). arXiv:1212.4524 [hep-ex]

[68] T. Horn et al. (Jefferson Lab F(pi)-2): "Determination of the Charged Pion Form Factor at $Q^2 = 1.60$ and 2.45-$(GeV/c)^2$". *Phys.Rev.Lett.* **97**, 192001 (2006). arXiv:nucl-ex/0607005

[69] V. Tadevosyan et al. (Jefferson Lab F(pi)): "Determination of the pion charge form-factor for $Q^2 = 0.60$-GeV^2 - 1.60-GeV^2". *Phys.Rev.* **C75**, 055205 (2007). arXiv:nucl-ex/0607007

[70] G. Huber et al. (Jefferson Lab): "Charged pion form-factor between $Q^2 = 0.60$-GeV^2 and 2.45-GeV^2. II. Determination of, and results for, the pion form-factor". *Phys.Rev.* **C78**, 045203 (2008). arXiv:0809.3052 [nucl-ex]

[71] K. K. Seth et al.: "Electromagnetic Structure of the Proton, Pion, and Kaon by High-Precision Form Factor Measurements at Large Timelike Momentum Transfers". *Phys.Rev.Lett.* **110**.2, 022002 (2013). arXiv:1210.1596 [hep-ex]

[72] S. J. Brodsky, F.-G. Cao, and G. F. de Teramond: "Meson Transition Form Factors in Light-Front Holographic QCD". *Phys. Rev.* **D84**, 075012 (2011). arXiv:1105.3999 [hep-ph]

[73] V. Punjabi et al.: "The Structure of the Nucleon: Elastic Electromagnetic Form Factors" (2015). arXiv:1503.01452 [nucl-ex]

[74] F. Ernst, R. Sachs, and K. Wali: "Electromagnetic form factors of the nucleon". *Phys.Rev.* **119**, 1105–1114 (1960)

[75] J. J. Kelly: "Nucleon charge and magnetization densities from Sachs form-factors". *Phys.Rev.* **C66**, 065203 (2002). arXiv:hep-ph/0204239

[76] R. Sachs: "High-Energy Behavior of Nucleon Electromagnetic Form Factors". *Phys.Rev.* **126**, 2256–2260 (1962)

[77] S. Collins et al.: "Dirac and Pauli form factors from lattice QCD". *Phys.Rev.* **D84**, 074507 (2011). arXiv:1106.3580 [hep-lat]

[78] T. Gutsche et al.: "Light-front quark model consistent with Drell-Yan-West duality and quark counting rules". *Phys.Rev.* **D89**.5, 054033 (2014). arXiv:1306.0366 [hep-ph]

[79] M. Diehl: "Generalized parton distributions from form-factors". *Nucl.Phys.Proc.Suppl.* **161**, 49–58 (2006). arXiv:hep-ph/0510221

[80] M. A. B. Bég, B. W. Lee, and A. Pais: "SU(6) and Electromagnetic Interactions". *Phys. Rev. Lett.* **13**, 514–517 (16 1964)

[81] P. J. Mohr, B. N. Taylor, and D. B. Newell: "CODATA Recommended Values of the Fundamental Physical Constants: 2010". *Rev.Mod.Phys.* **84**, 1527–1605 (2012). arXiv:1203.5425 [physics.atom-ph]

[82] J. Arrington: "How well do we know the electromagnetic form-factors of the proton?" *Eur.Phys.J.* **A17**, 311–315 (2003). arXiv:hep-ph/0209243

[83] P. Blunden, W. Melnitchouk, and J. Tjon: "Two-photon exchange in elastic electron-nucleon scattering". *Phys.Rev.* **C72**, 034612 (2005). arXiv:nucl-th/0506039

[84] R. Pohl et al.: "The size of the proton". *Nature* **466**, 213–216 (2010)

[85] A. Antognini et al.: "Proton Structure from the Measurement of $2S - 2P$ Transition Frequencies of Muonic Hydrogen". *Science* **339**, 417–420 (2013)

[86] P. A. R. Ade et al. (Planck): "Planck 2015 results. XIII. Cosmological parameters" (2015). arXiv:1502.01589 [astro-ph.CO]

[87] R. Bernabei et al. (DAMA Collaboration): "First results from DAMA/LIBRA and the combined results with DAMA/NaI". *Eur.Phys.J.* **C56**, 333–355 (2008). arXiv:0804.2741 [astro-ph]

[88] C. E. Aalseth et al. (CoGeNT Collaboration): "Search for an Annual Modulation in a p-Type Point Contact Germanium Dark Matter Detector". *Physical Review Letters* **107**.14, 141301 (2011). arXiv:1106.0650 [astro-ph.CO]

[89] E. Aprile et al. (XENON100 Collaboration): "Dark Matter Results from 225 Live Days of XENON100 Data". *Phys.Rev.Lett.* **109**, 181301 (2012). arXiv:1207.5988 [astro-ph.CO]

[90] F. Zwicky: "Die Rotverschiebung von extragalaktischen Nebeln". *Helv. Phys. Acta* **6**, 110–127 (1933)

[91] R. Fusco-Femiano and J. P. Hughes: "Nonpolytropic Model for the Coma Cluster". *Astrophys. J.* **429**, 545 (1994)

[92] A. Del Popolo: "Nonbaryonic Dark Matter in Cosmology". *Int.J.Mod.Phys.* **D23**, 1430005 (2014). arXiv:1305.0456 [astro-ph.CO]

[93] D. Clowe et al.: "A direct empirical proof of the existence of dark matter". *Astrophys. J.* **648**, L109 (2006). arXiv:astro-ph/0608407

[94] M. Bradac et al.: "Revealing the properties of dark matter in the merging cluster MACSJ0025.4-1222". *Astrophys. J.* **687**, 959 (2008). arXiv:0806.2320 [astro-ph]

[95] M. Roos: "Dark Matter: The evidence from astronomy, astrophysics and cosmology" (2010). arXiv:1001.0316 [astro-ph.CO]

[96] P. Tisserand et al.: "Limits on the Macho Content of the Galactic Halo from the EROS-2 Survey of the Magellanic Clouds". *Astron. Astrophys.* **469**, 387–404 (2007). arXiv:astro-ph/0607207

[97] J. R. Primack: "Dark matter and structure formation". *Midrasha Mathematicae in Jerusalem: Winter School in Dynamical Systems Jerusalem, Israel, January 12-17, 1997*. 1997. arXiv:astro-ph/9707285. URL: http://alice.cern.ch/format/showfull?sysnb=0254285

[98] B. Moore: "Evidence against dissipationless dark matter from observations of galaxy haloes". *Nature* **370**, 629 (1994)

[99] R. A. Flores and J. R. Primack: "Observational and theoretical constraints on singular dark matter halos". *Astrophys. J.* **427**, L1–4 (1994). arXiv:astro-ph/9402004

[100] K. A. Oman et al.: "The unexpected diversity of dwarf galaxy rotation curves" (2015). arXiv:1504.01437 [astro-ph.GA]

[101] D. B. Kaplan: "Single explanation for both baryon and dark matter densities". *Phys. Rev. Lett.* **68**, 741–743 (6 1992). URL: http://link.aps.org/doi/10.1103/PhysRevLett.68.741

[102] J. M. Cline et al.: "Composite strongly interacting dark matter". *Phys.Rev.* **D90**.1, 015023 (2014). arXiv:1312.3325 [hep-ph]

[103] T. Appelquist et al. (Lattice Strong Dynamics (LSD) Collaboration): "Lattice calculation of composite dark matter form factors". *Phys.Rev.* **D88**.1, 014502 (2013). arXiv:1301.1693 [hep-ph]

[104] S. Nussinov: "Technocosmology — could a technibaryon excess provide a "natural" missing mass candidate?" *Physics Letters B* **165**.1–3, 55 (1985)

[105] R. Chivukula and T. P. Walker: "Technicolor cosmology". *Nuclear Physics B* **329**.2, 445 –463 (1990)

[106] R. S. Chivukula et al.: "A Comment on the strong interactions of color - neutral technibaryons". *Phys. Lett.* **B298**, 380–382 (1993). arXiv:hep-ph/9210274

[107] J. Bagnasco, M. Dine, and S. D. Thomas: "Detecting technibaryon dark matter". *Phys. Lett.* **B320**, 99–104 (1994). arXiv:hep-ph/9310290 [hep-ph]

[108] T. Banks, J. D. Mason, and D. O'Neil: "A Dark matter candidate with new strong interactions". *Phys. Rev.* **D72**, 043530 (2005). arXiv:hep-ph/0506015

[109] D. E. Kaplan et al.: "Atomic Dark Matter". *JCAP* **1005**, 021 (2010). arXiv:0909.0753 [hep-ph]

[110] S. R. Behbahani et al.: "Nearly Supersymmetric Dark Atoms". *Adv. High Energy Phys.* **2011**, 709492 (2011). arXiv:1009.3523 [hep-ph]

[111] D. E. Kaplan et al.: "Dark Atoms: Asymmetry and Direct Detection". *JCAP* **1110**, 011 (2011). arXiv:1105.2073 [hep-ph]

[112] J. M. Cline, Z. Liu, and W. Xue: "Millicharged Atomic Dark Matter". *Phys. Rev.* **D85**, 101302 (2012). arXiv:1201.4858 [hep-ph]

[113] F.-Y. Cyr-Racine and K. Sigurdson: "Cosmology of Atomic Dark Matter". *Phys. Rev. D* **87**, 103515 (2013). arXiv:1209.5752 [astro-ph.CO]

[114] T. Banks, J.-F. Fortin, and S. Thomas: "Direct Detection of Dark Matter Electromagnetic Dipole Moments" (2010). arXiv:1007.5515 [hep-ph]

[115] J. D. Lewin and P. F. Smith: "Review of mathematics, numerical factors, and corrections for dark matter experiments based on elastic nuclear recoil". *Astropart. Phys.* **6**, 87–112 (1996)

[116] K. Choi, C. Rott, and Y. Itow: "Impact of the dark matter velocity distribution on capture rates in the Sun". *JCAP* **1405**, 049 (2014). arXiv:1312.0273 [astro-ph.HE]

[117] E. Aprile et al. (XENON100): "Limits on spin-dependent WIMP-nucleon cross sections from 225 live days of XENON100 data". *Phys.Rev.Lett.* **111**.2, 021301 (2013). arXiv:1301.6620 [astro-ph.CO]

[118] W. M. Haynes: *CRC handbook of chemistry and physics*. 96th ed. CRC press, 2015

Appendix A

Tables of Particles

All data are from Particle Data Group (reference [28]). Here, only 3- and 4-star mesons and baryons are included. In reference [28], the masses of baryons are given as limits and an estimate. Here they are transferred to the $\pm$ form for clarity and compactness. Because of the limited precision of the light-front methods used here, all masses are rounded to the nearest MeV, thus practically diminishing the errors in the masses of $\pi(140)$ and $\rho(770)$ to zero.

The radial quantum number n, internal spin S and internal orbital angular momentum L of the baryons are deduced from the total angular momentum and parity of the PDG by using the $\mathrm{SU}(6)\supset\mathrm{SU}(3)_{\mathrm{flavour}}\otimes\mathrm{SU}(2)_{\mathrm{spin}}$ multiplet structure presented in e.g. reference [39].

Name	Mass (MeV)	J^P	n	L	S
$\pi(140)$	140	0^-	0	0	0
$b_1(1235)$	1230 ± 4	1^+	0	1	0
$\pi_2(1670)$	1672 ± 3	2^-	0	2	0
$\pi(1300)$	1300 ± 100	0^-	1	0	0
$\pi(1800)$	1812 ± 12	0^-	2	0	0
$\pi_2(1880)$	1895 ± 16	2^-	1	2	0

Table A.1: Confirmed pseudoscalar mesons with a hypercharge $I = 1$. The quantum numbers n, L and S are the radial quantum number, the orbital angular momentum and spin respectively.

Name	Mass (MeV)	J^P	n	L	S
$\rho(770)$	775	1^-	0	0	1
$a_0(980)$	980 ± 20	0^+	0	1	1
$a_1(1260)$	1230 ± 40	1^+	0	1	1
$a_2(1320)$	1318 ± 1	2^+	0	1	1
$\rho(1450)$	1465 ± 25	1^-	1	1	0
$\rho(1700)$	1720 ± 20	1^-	2	1	0
$\rho_3(1690)$	1689 ± 2	3^-	0	2	1
$a_4(2040)$	1996^{+10}_{-9}	4^+	0	2	1

Table A.2: Confirmed vector mesons with a hypercharge $I = 1$.

Name	Mass (MeV)	J^P	n	L	S
$N(940)$	939	$1/2^+$	0	0	1/2
$N(1440)$	1430 ± 20	$1/2^+$	1	0	1/2
$N(1520)$	1515 ± 5	$3/2^-$	0	1	1/2
$N(1535)$	1535 ± 10	$1/2^-$	0	1	1/2
$N(1650)$	1655^{+15}_{-10}	$1/2^-$	0	1	3/2
$N(1675)$	1675 ± 5	$5/2^-$	0	1	3/2
$N(1680)$	1685 ± 5	$5/2^+$	0	2	1/2
$N(1700)$	1700 ± 50	$3/2^-$	0	1	3/2
$N(1710)$	1710 ± 30	$1/2^+$	2	0	1/2
$N(1720)$	1720^{+30}_{-20}	$3/2^+$	0	2	1/2
$N(1875)$	1875^{+45}_{-55}	$3/2^-$	1	1	3/2
$N(1900)$	1900	$3/2^+$	1	2	1/2
$N(2190)$	2190^{+10}_{-90}	$7/2^-$	0	3	3/2
$N(2220)$	2250 ± 50	$9/2^+$	0	4	1/2
$N(2250)$	2275 ± 75	$9/2^-$	0	3	3/2
$N(2600)$	2600 ± 50	$11/2^-$	0	5	3/2

Table A.3: Confirmed nucleon resonances, i.e. $s = 0$ and $I = 1/2$ baryon resonances.

Name	Mass (MeV)	J^P	n	L	S
$\Delta(1232)$	1232 ± 2	$3/2^+$	0	0	3/2
$\Delta(1600)$	1600 ± 100	$3/2^+$	1	0	3/2
$\Delta(1620)$	1630 ± 30	$1/2^-$	0	1	1/2
$\Delta(1700)$	1700^{+50}_{-30}	$3/2^-$	0	1	1/2
$\Delta(1905)$	1880^{+30}_{-25}	$5/2^+$	0	2	3/2
$\Delta(1910)$	1890^{+20}_{-30}	$1/2^+$	0	2	3/2
$\Delta(1920)$	1920^{+50}_{-20}	$3/2^+$	0	2	3/2
$\Delta(1930)$	1950 ± 50	$5/2^-$	1	1	3/2
$\Delta(1950)$	1930^{+20}_{-15}	$7/2^+$	0	2	3/2
$\Delta(2420)$	2420^{+80}_{-120}	$11/2^+$	0	4	3/2

Table A.4: Confirmed Δ resonances, i.e. $s = 0$ and $I = 3/2$ baryon resonances.